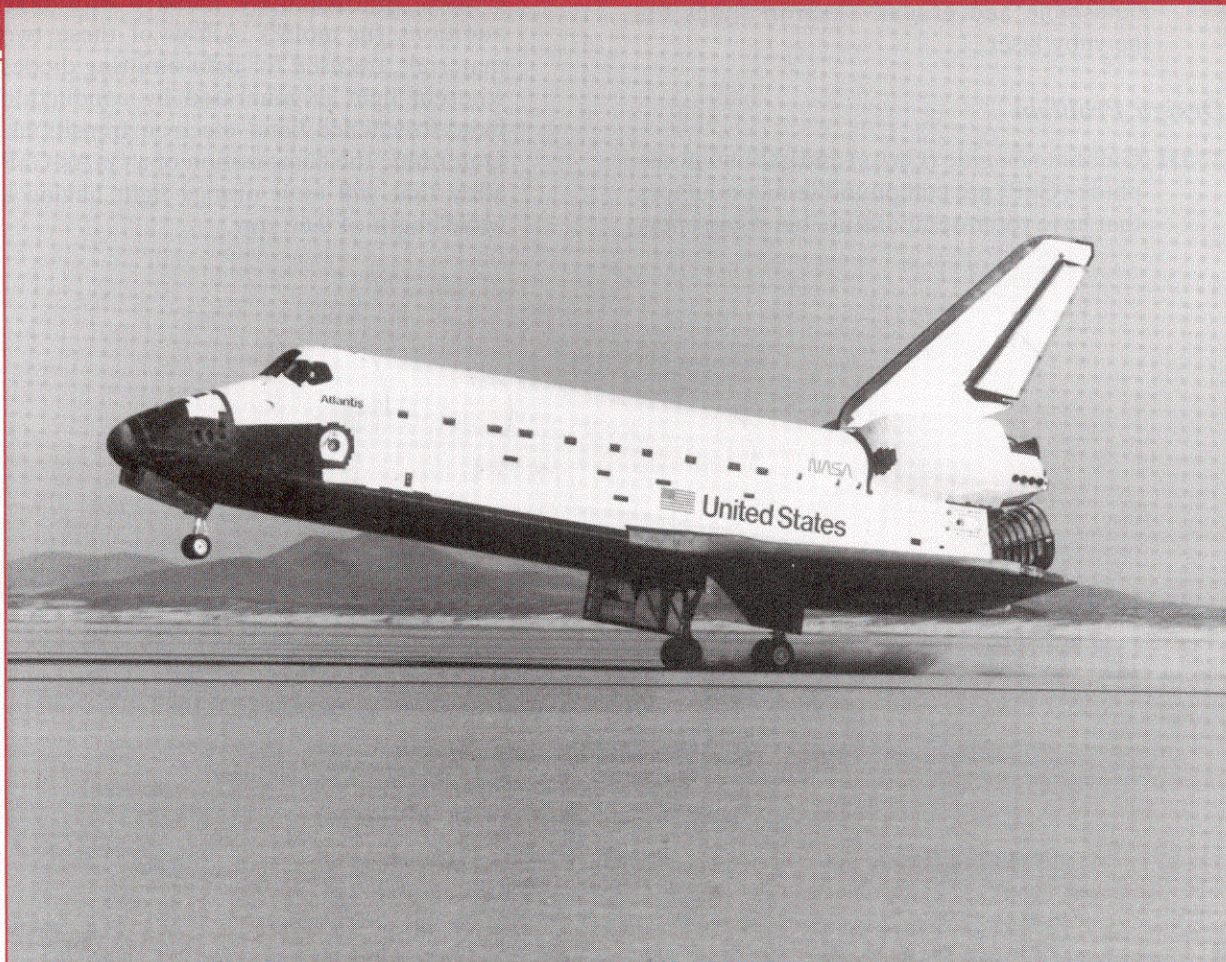


Chapter 23 / Materials Selection and Design Considerations



Shown in this photograph is the landing of the *Atlantis* Space Shuttle Orbiter. This chapter discusses the materials that are used for its outer airframe's thermal protection system. [Photograph courtesy the National Aeronautics and Space Administration (NASA).]

Why Study Materials Selection and Design Considerations?

Perhaps one of the most important tasks that an engineer may be called upon to perform is that of materials selection with regard to component design. Inappropriate or improper decisions can be disastrous from both economic and safety perspectives. Therefore, it is essential that the engineering stu-

dent become familiar with and versed in the procedures and protocols that are normally employed in this process. This chapter discusses materials selection issues in several contexts and from various perspectives.

Learning Objectives

After careful study of this chapter you should be able to do the following:

1. Describe how the strength performance index for a solid cylindrical shaft is determined.
2. Describe the manner in which materials selection charts are employed in the materials selection process.
3. Briefly describe the steps that are used to ascertain whether or not a particular metal alloy is suitable for use in an automobile valve spring.
4. List and briefly explain six biocompatibility considerations relative to materials that are employed in artificial hip replacements.
5. Name the four components found in the artificial hip replacement, and, for each, list its specific material requirements.
6. (a) Name the three components of the thermal protection system for the Space Shuttle Orbiter. (b) Describe the composition, microstructure, and general properties of the ceramic tiles that are used on the Space Shuttle Orbiter.
7. Describe the components and their functions for an integrated circuit leadframe.
8. (a) Name and briefly describe the three processes that are carried out during integrated circuit packaging. (b) Note property requirements for each of these processes, and, in addition, cite at least two materials that are employed.

23.1 INTRODUCTION

Virtually the entire book to this point has dealt with the properties of various materials, how the properties of a specific material are dependent on its structure, and, in many cases, how structure may be fashioned by the processing technique that is employed during production. Of late, there has been a trend to emphasize the element of *design* in engineering pedagogy. To a materials scientist or materials engineer, design can be taken in several contexts. First of all, it can mean designing new materials having unique property combinations. Alternatively, design can involve selecting a new material having a better combination of characteristics for a specific application; choice of material cannot be made without consideration of necessary manufacturing processes (e.g., forming, welding, etc.), which also rely on material properties. Or, finally, design might mean developing a process for producing a material having better properties.

One particularly effective technique for teaching design principles is the case study method. With this technique, the solutions to real-life engineering problems are carefully analyzed in detail so that the student may observe the procedures and rationale that are involved in the decision-making process. We have chosen to perform five case studies which draw upon principles that were introduced in previous chapters. These five studies involve materials that are used for the following: (1) a torsionally stressed cylindrical shaft; (2) an automobile valve spring; (3) the artificial total hip replacement; (4) the thermal protection system on the Space Shuttle Orbiter; and (5) integrated circuit packages.

MATERIALS SELECTION FOR A TORSIONALLY STRESSED CYLINDRICAL SHAFT

We begin by addressing the design process from the perspective of materials selection; that is, for some application, selecting a material having a desirable or optimum property or combination of properties. Elements of this materials selection process involve deciding on the constraints of the problem, and, from these, establishing criteria that can be used in materials selection to maximize performance.

The component or structural element we have chosen to discuss is a solid

cylindrical shaft that is subjected to a torsional stress. Strength of the shaft will be considered in detail, and criteria will be developed for the maximization of strength with respect to both minimum material mass and minimum cost. Other parameters and properties that may be important in this selection process are also discussed briefly.

23.2 STRENGTH

For this portion of the problem, we will establish a criterion for selection of light and strong materials for this shaft. It will be assumed that the twisting moment and length of the shaft are specified, whereas the radius (or cross-sectional area) may be varied. We develop an expression for the mass of material required in terms of twisting moment, shaft length, and density and strength of the material. Using this expression, it will be possible to evaluate the performance—that is, maximize the strength of this torsionally stressed shaft with respect to mass and, in addition, relative to material cost.

Consider the cylindrical shaft of length L and radius r , as shown in Figure 23.1. The application of twisting moment (or torque), M_t , produces an angle of twist ϕ . Shear stress τ at radius r is defined by the equation

$$\tau = \frac{M_t r}{J} \quad (23.1)$$

Here, J is the polar moment of inertia, which for a solid cylinder is

$$J = \frac{\pi r^4}{2} \quad (23.2)$$

Thus,

$$\tau = \frac{2M_t}{\pi r^3} \quad (23.3)$$

A safe design calls for the shaft to be able to sustain some twisting moment without fracture. In order to establish a materials selection criterion for a light and strong material, we replace the shear stress in Equation 23.3 with the shear strength of the material τ_f divided by a factor of safety N , as

$$\frac{\tau_f}{N} = \frac{2M_t}{\pi r^3} \quad (23.4)$$

It is now necessary to take into consideration material mass. The mass m of any given quantity of material is just the product of its density (ρ) and volume. Since the volume of a cylinder is just $\pi r^2 L$, then

$$m = \pi r^2 L \rho \quad (23.5)$$

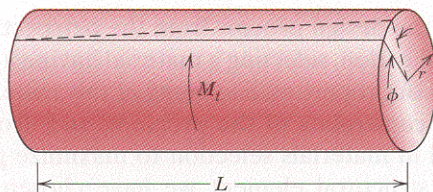


FIGURE 23.1 A solid cylindrical shaft that experiences an angle of twist ϕ in response to the application of a twisting moment M_t .

Or, the radius of the shaft in terms of its mass is just

$$r = \sqrt{\frac{m}{\pi L \rho}} \quad (23.6)$$

Substitution of this r expression into Equation 23.4 leads to

$$\begin{aligned} \frac{\tau_f}{N} &= \frac{2M_t}{\pi \left(\sqrt{\frac{m}{\pi L \rho}} \right)^3} \\ &= 2M_t \sqrt{\frac{\pi L^3 \rho^3}{m^3}} \end{aligned} \quad (23.7)$$

Solving this expression for the mass m yields

$$m = (2NM_t)^{2/3} (\pi^{1/3} L) \left(\frac{\rho}{\tau_f^{2/3}} \right) \quad (23.8)$$

The parameters on the right-hand side of this equation are grouped into three sets of parentheses. Those contained within the first set (i.e., N and M_t) relate to the safe functioning of the shaft. Within the second parentheses is L , a geometric parameter. And, finally, the material properties of density and strength are contained within the last set.

The upshot of Equation 23.8 is that the best materials to be used for a light shaft which can safely sustain a specified twisting moment are those having low $\rho/\tau_f^{2/3}$ ratios. In terms of material suitability, it is sometimes preferable to work with what is termed a *performance index*, P , which is just the reciprocal of this ratio; that is

$$P = \frac{\tau_f^{2/3}}{\rho} \quad (23.9)$$

In this context we want to utilize a material having a large performance index.

At this point it becomes necessary to examine the performance indices of a variety of potential materials. This procedure is expedited by the utilization of what are termed *materials selection charts*.¹ These are plots of the values of one material property versus those of another property. Both axes are scaled logarithmically and usually span about five orders of magnitude, so as to include the properties of virtually all materials. For example, for our problem, the chart of interest is logarithm of strength versus logarithm of density, which is shown in Figure 23.2.² It may be noted on this plot that materials of a particular type (e.g., woods, engineering polymers, etc.) cluster together and are enclosed within an envelope delineated with a bold line. Subclasses within these clusters are enclosed using finer lines.

¹ A comprehensive collection of these charts may be found in M. F. Ashby, *Materials Selection in Mechanical Design*, Pergamon Press, Oxford, 1992.

² Strength for metals and polymers is taken as yield strength, for ceramics and glasses, compressive strength, for elastomers, tear strength, and for composites, tensile failure strength.

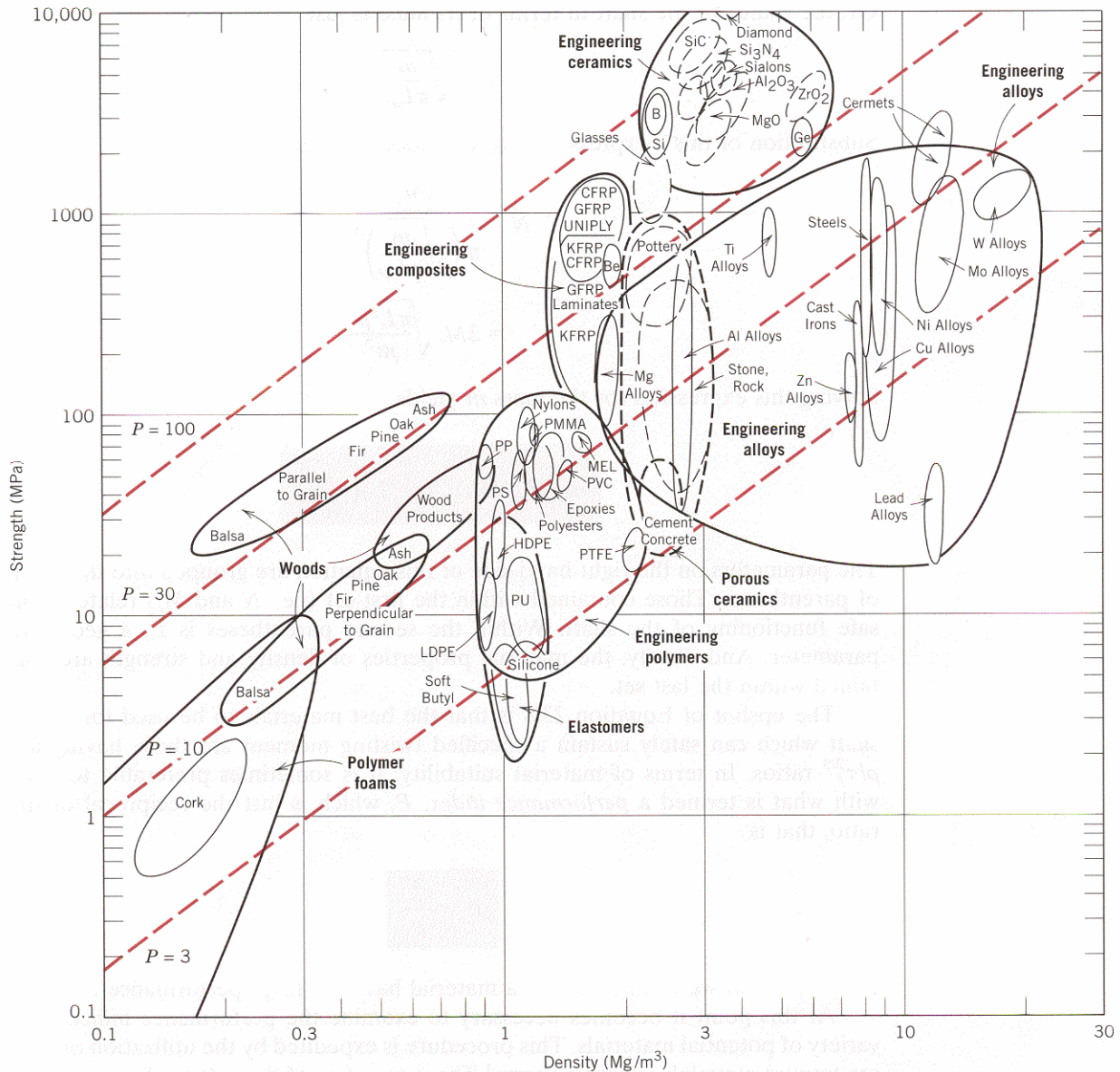


FIGURE 23.2 Strength versus density materials selection chart. Design guidelines for performance indices of 3, 10, 30, and 100 $(\text{MPa})^{2/3}\text{m}^3/\text{Mg}$ have been constructed, all having a slope of $\frac{2}{3}$. (Adapted from M. F. Ashby, *Materials Selection in Mechanical Design*. Copyright © 1992. Reprinted by permission of Butterworth-Heinemann Ltd.)

Now, taking the logarithm of both sides of Equation 23.9 and rearranging yields

$$\log \tau_f = \frac{2}{3} \log \rho + \frac{2}{3} \log P \quad (23.10)$$

This expression tells us that a plot of $\log \tau_f$ versus $\log \rho$ will yield a family of straight and parallel lines all having a slope of $\frac{2}{3}$; each line in the family corresponds to a different performance index, P . These lines are termed *design guidelines*, and four have been included in Figure 23.2 for P values of 3, 10, 30, and 100 $(\text{MPa})^{2/3}\text{m}^3/\text{Mg}$. All materials that lie on one of these lines will perform equally well in terms

of strength-per-mass basis; materials whose positions lie above a particular line will have higher performance indices, while those lying below will exhibit poorer performances. For example, a material on the $P = 30$ line will yield the same strength with one-third the mass as another material that lies along the $P = 10$ line.

The selection process now involves choosing one of these lines, a “selection line” that includes some subset of these materials; for the sake of argument let us pick $P = 10$ $(\text{MPa})^{2/3} \text{m}^3/\text{Mg}$, which is represented in Figure 23.3. Materials lying

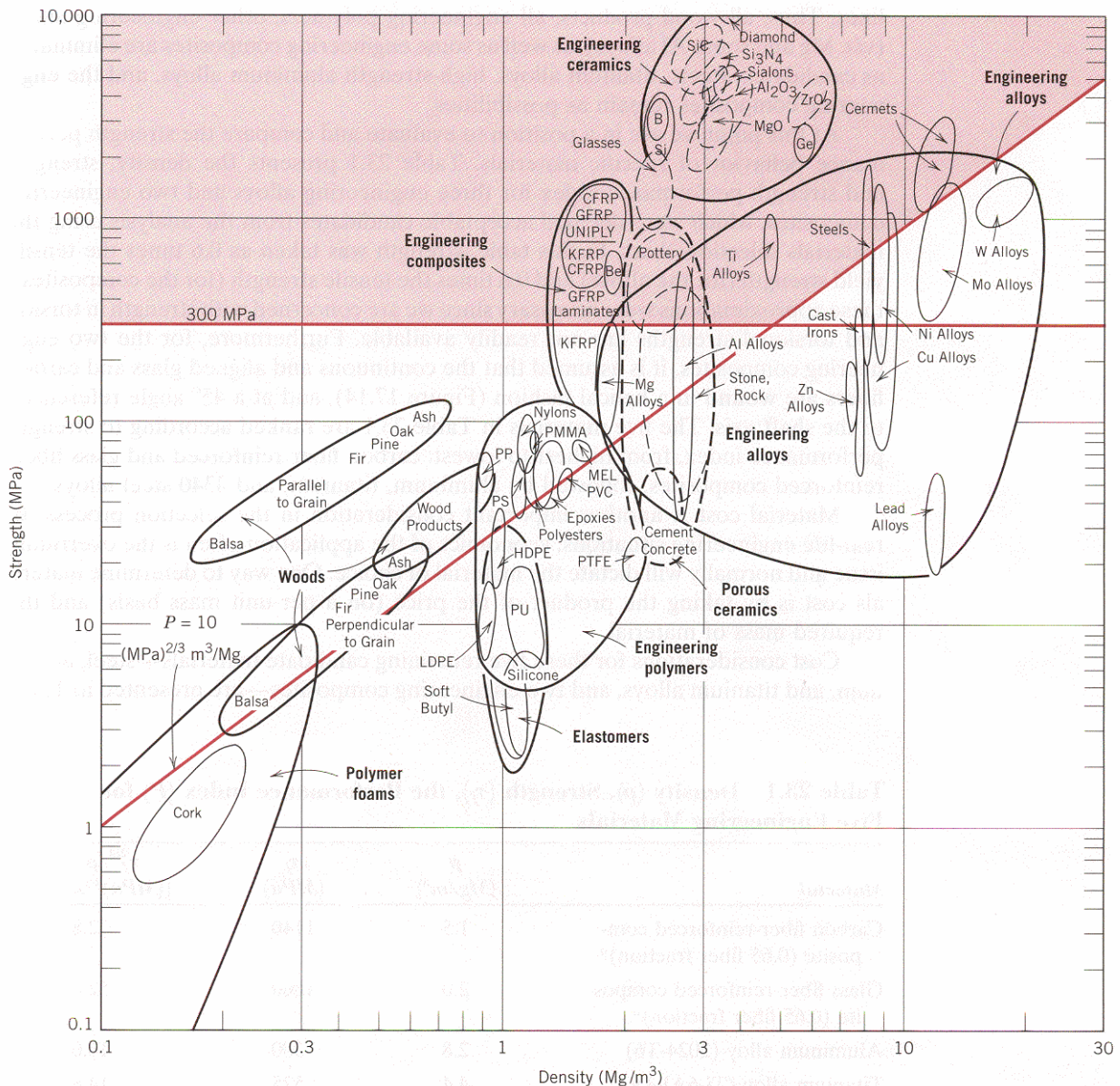


FIGURE 23.3 Strength versus density materials selection chart. Those materials lying within the shaded region are acceptable candidates for a solid cylindrical shaft which has a mass-strength performance index in excess of 10 $(\text{MPa})^{2/3} \text{m}^3/\text{Mg}$, and a strength of at least 300 MPa (43,500 psi). (Adapted from M. F. Ashby, *Materials Selection in Mechanical Design*. Copyright © 1992. Reprinted by permission of Butterworth-Heinemann Ltd.)

along this line or above it are in the “search region” of the diagram and are possible candidates for this rotating shaft. These include wood products, some plastics, a number of engineering alloys, the engineering composites, and glasses and engineering ceramics. On the basis of fracture toughness considerations, the engineering ceramics and glasses are ruled out as possibilities.

Let us now impose a further constraint on the problem, namely that the strength of the shaft must equal or exceed 300 MPa (43,500 psi). This may be represented on the materials selection chart by a horizontal line constructed at 300 MPa, Figure 23.3. Now the search region is further restricted to that area above both of these lines. Thus, all wood products, all engineering polymers, other engineering alloys (viz. Mg and some Al alloys), as well as some engineering composites are eliminated as candidates; steels, titanium alloys, high-strength aluminum alloys, and the engineering composites remain as possibilities.

At this point we are in a position to evaluate and compare the strength performance behavior of specific materials. Table 23.1 presents the density, strength, and strength performance index for three engineering alloys and two engineering composites, which were deemed acceptable candidates from the analysis using the materials selection chart. In this table, strength was taken as 0.6 times the tensile yield strength (for the alloys) and 0.6 times the tensile strength (for the composites); these approximations were necessary since we are concerned with strength in torsion and torsional strengths are not readily available. Furthermore, for the two engineering composites, it is assumed that the continuous and aligned glass and carbon fibers are wound in a helical fashion (Figure 17.14), and at a 45° angle referenced to the shaft axis. The five materials in Table 23.1 are ranked according to strength performance index, from highest to lowest: carbon fiber-reinforced and glass fiber-reinforced composites, followed by aluminum, titanium, and 4340 steel alloys.

Material cost is another important consideration in the selection process. In real-life engineering situations, economics of the application often is the overriding issue and normally will dictate the material of choice. One way to determine materials cost is by taking the product of the price (on a per-unit mass basis) and the required mass of material.

Cost considerations for these five remaining candidate materials—steel, aluminum, and titanium alloys, and two engineering composites—are presented in Table

Table 23.1 Density (ρ), Strength (τ_f), the Performance Index (P) for Five Engineering Materials

Material	ρ (Mg/m ³)	τ_f (MPa)	$\frac{\tau_f^{2/3}}{\rho} = P$ [(MPa) ^{2/3} m ³ /Mg]
Carbon fiber-reinforced composite (0.65 fiber fraction) ^a	1.5	1140	72.8
Glass fiber-reinforced composite (0.65 fiber fraction) ^a	2.0	1060	52.0
Aluminum alloy (2024-T6)	2.8	300	16.0
Titanium alloy (Ti-6Al-4V)	4.4	525	14.8
4340 Steel (oil-quenched and tempered)	7.8	780	10.9

^a The fibers in these composites are continuous, aligned, and wound in a helical fashion at a 45° angle relative to the shaft axis.

Table 23.2 Tabulation of the $\rho/\tau_f^{2/3}$ Ratio, Relative Cost (\bar{c}), and the Product of $\rho/\tau_f^{2/3}$ and \bar{c} for Five Engineering Materials^a

Material	$\rho/\tau_f^{2/3}$ [$10^{-2} \{ \text{Mg}/(\text{MPa})^{2/3} \text{m}^3 \}$]	\bar{c} (\$/\$)	$\bar{c}(\rho/\tau_f^{2/3})$ [$10^{-2} (\text{\$/\$}) \{ \text{Mg}/(\text{MPa})^{2/3} \text{m}^3 \}$]
4340 Steel (oil-quenched and tempered)	9.2	5	46
Glass fiber-reinforced composite (0.65 fiber fraction) ^b	1.9	40	76
Aluminum alloy (2024-T6)	6.2	15	93
Carbon fiber-reinforced composite (0.65 fiber fraction) ^b	1.4	80	112
Titanium alloy (Ti-6Al-4V)	6.8	110	748

^a The relative cost is the ratio of the prices per unit mass of the material and low-carbon steel.

^b The fibers in these composites are continuous, aligned, and wound in a helical fashion at a 45° angle relative to the shaft axis.

23.2. In the first column is tabulated $\rho/\tau_f^{2/3}$. The next column lists the approximate relative cost, denoted as \bar{c} ; this parameter is simply the per-unit mass cost of material divided by the per-unit mass cost for low-carbon steel, one of the common engineering materials. The underlying rationale for using \bar{c} is that while the price of a specific material will vary over time, the price ratio between that material and another will, most likely, change more slowly.

Finally, the right-hand column of Table 23.2 shows the product of $\rho/\tau_f^{2/3}$ and \bar{c} . This product provides a comparison of these several materials on the basis of the cost of materials for a cylindrical shaft that would not fracture in response to the twisting moment M_t . We use this product inasmuch as $\rho/\tau_f^{2/3}$ is proportional to the mass of material required (Equation 23.8) and \bar{c} is the relative cost on a per-unit mass basis. Now the most economical is the 4340 steel, followed by the glass fiber-reinforced composite, 2024-T6 aluminum, the carbon fiber-reinforced composite, and the titanium alloy. Thus, when the issue of economics is considered, there is a significant alteration within the ranking scheme. For example, inasmuch as the carbon fiber-reinforced composite is relatively expensive, it is significantly less desirable; or, in other words, the higher cost of this material may not outweigh the enhanced strength it provides.

23.3 OTHER PROPERTY CONSIDERATIONS AND THE FINAL DECISION

To this point in our materials selection process we have considered only the strength of materials. Other properties relative to the performance of the cylindrical shaft may be important—for example, stiffness, and, if the shaft rotates, fatigue behavior. Furthermore, fabrication costs should also be considered; in our analysis they have been neglected.

Relative to stiffness, a stiffness-to-mass performance analysis similar to that above could be conducted. For this case, the stiffness performance index P_s is

$$P_s = \frac{\sqrt{G}}{\rho} \quad (23.11)$$

where G is the shear modulus. The appropriate materials selection chart ($\log G$ versus $\log \rho$) would be used in the preliminary selection process. Subsequently, performance index and per-unit-mass cost data would be collected on specific candidate materials; from these analyses the materials would be ranked on the basis of stiffness performance and cost.

In deciding on the best material, it may be worthwhile to make a table employing the results of the various criteria that were used. The tabulation would include, for all candidate materials, performance index, cost, etc. for each criterion, as well as comments relative to any other important considerations. This table puts in perspective the important issues and facilitates the final decision process.

AUTOMOBILE VALVE SPRING

23.4 INTRODUCTION

The basic function of a spring is to store mechanical energy as it is initially elastically deformed and then recoup this energy at a later time as the spring recoils. In this section helical springs that are used in mattresses and in retractable pens and as suspension springs in automobiles are discussed. A stress analysis will be conducted on this type of spring, and the results will then be applied to a valve spring that is utilized in automobile engines.

Consider the helical spring shown in Figure 23.4, which has been constructed of wire having a circular cross section of diameter d ; the coil center-to-center diameter is denoted as D . The application of a compressive force F causes a twisting force, or moment, denoted as T , as shown in the figure. A combination of shear stresses result, the sum of which, τ , is

$$\tau = \frac{8FD}{\pi d^3} K_w \quad (23.12)$$

where K_w is a force-independent constant that is a function of the D/d ratio:

$$K_w = 1.60 \left(\frac{D}{d} \right)^{-0.140} \quad (23.13)$$

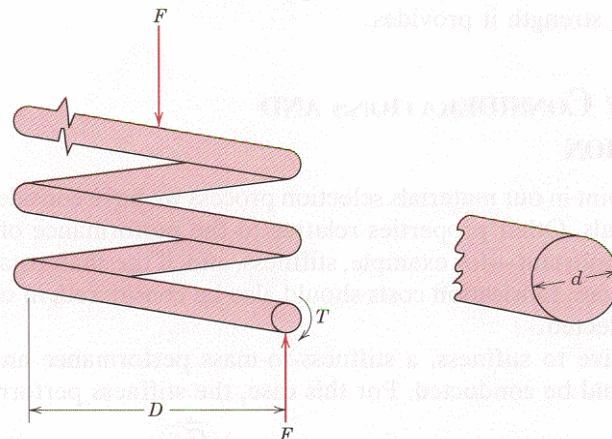


FIGURE 23.4 Schematic diagram of a helical spring showing the twisting moment T that results from the compressive force F . (Adapted from K. Edwards and P. McKee, *Fundamentals of Mechanical Component Design*. Copyright © 1991 by McGraw-Hill, Inc. Reproduced with permission of The McGraw-Hill Companies.)

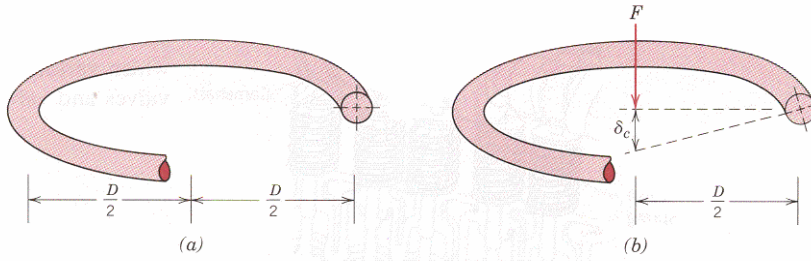


FIGURE 23.5 Schematic diagrams of one coil of a helical spring, (a) prior to being compressed, and (b) showing the deflection δ_c produced from the compressive force F . (Adapted from K. Edwards and P. McKee, *Fundamentals of Mechanical Component Design*. Copyright © 1991 by McGraw-Hill, Inc. Reproduced with permission of The McGraw-Hill Companies.)

In response to the force F , the coiled spring will experience deflection, which will be assumed to be totally elastic. The amount of deflection per coil of spring, δ_c , as indicated in Figure 23.5, is given by the expression

$$\delta_c = \frac{8FD^3}{d^4G} \quad (23.14)$$

where G is the shear modulus of the material from which the spring is constructed. Furthermore, δ_c may be computed from the total spring deflection, δ_s , and the number of effective spring coils, N_c , as

$$\delta_c = \frac{\delta_s}{N_c} \quad (23.15)$$

Now, solving for F in Equation 23.14 gives

$$F = \frac{d^4\delta_c G}{8D^3} \quad (23.16)$$

and substituting for F in Equation 23.12 leads to

$$\tau = \frac{\delta_c G d}{\pi D^2} K_w \quad (23.17)$$

Under normal circumstances, it is desired that a spring experience no permanent deformation upon loading; this means that the right-hand side of Equation 23.17 must be less than the shear yield strength τ_y of the spring material, or that

$$\tau_y > \frac{\delta_c G d}{\pi D^2} K_w \quad (23.18)$$

23.5 AUTOMOBILE VALVE SPRING

We shall now apply the results of the preceding section to an automobile valve spring. A cut-away schematic diagram of an automobile engine showing these springs is presented in Figure 23.6. Functionally, springs of this type permit both

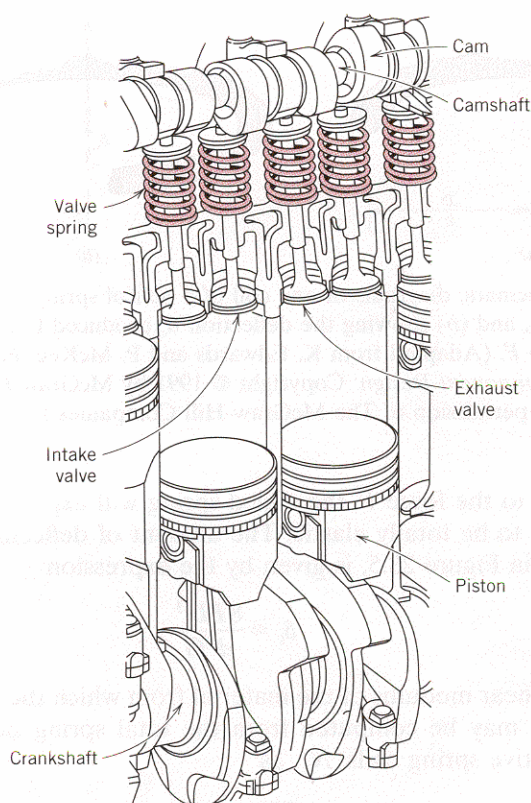


FIGURE 23.6 Cutaway drawing of a section of an automobile engine in which various components including valves and valve springs are shown.

intake and exhaust valves to alternately open and close as the engine is in operation. Rotation of the camshaft causes a valve to open and its spring to be compressed, so that the load on the spring is increased. The stored energy in the spring then forces the valve to close as the camshaft continues its rotation. This process occurs for each valve for each engine cycle, and over the lifetime of the engine it occurs many millions of times. Furthermore, during normal engine operation, the temperature of the springs is approximately 80°C (175°F).

A photograph of a typical valve spring is shown in Figure 23.7. The spring has a total length of 1.67 in. (42 mm), is constructed of wire having a diameter d of 0.170 in. (4.3 mm), has six coils (only four of which are active), and has a center-to-center diameter D of 1.062 in. (27 mm). Furthermore, when installed and when a valve is completely closed, its spring is compressed a total of 0.24 in. (6.1 mm), which, from Equation 23.15, gives an installed deflection per coil δ_{ic} of

$$\delta_{ic} = \frac{0.24 \text{ in.}}{4 \text{ coils}} = 0.060 \text{ in./coil (1.5 mm/coil)}$$

The cam lift is 0.30 in. (7.6 mm), which means that when the cam completely opens a valve, the spring experiences a maximum total deflection equal to the sum of the valve lift and the compressed deflection, namely, 0.30 in. + 0.24 in. = 0.54 in. (13.7 mm). Hence, the maximum deflection per coil, δ_{mc} , is

$$\delta_{mc} = \frac{0.54 \text{ in.}}{4 \text{ coils}} = 0.135 \text{ in./coil (3.4 mm/coil)}$$

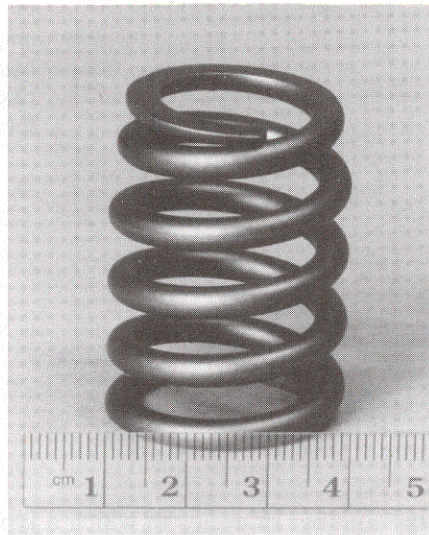


FIGURE 23.7 Photograph of a typical automobile valve spring.

Thus, we have available all of the parameters in Equation 23.18 (taking $\delta_c = \delta_{mc}$), except for τ_y , the required shear yield strength of the spring material.

However, the material parameter of interest is really not τ_y inasmuch as the spring is continually stress cycled as the valve opens and closes during engine operation; this necessitates designing against the possibility of failure by fatigue rather than against the possibility of yielding. This fatigue complication is handled by choosing a metal alloy that has a fatigue limit (Figure 8.22a) that is greater than the cyclic stress amplitude to which the spring will be subjected. For this reason, steel alloys, which have fatigue limits, are normally employed for valve springs.

When using steel alloys in spring design, two assumptions may be made if the stress cycle is reversed (if $\tau_m = 0$, where τ_m is the mean stress, or, equivalently, if $\tau_{\max} = -\tau_{\min}$, in accordance with Equation 8.21 and as noted in Figure 23.8). The first of these assumptions is that the fatigue limit of the alloy (expressed as stress amplitude) is 45,000 psi (310 MPa), the threshold of which occurs at about 10^6 cycles. Secondly, for torsion and on the basis of experimental data, it has been found that the fatigue strength at 10^3 cycles is $0.67TS$, where TS is the tensile strength of the material (as measured from a pure tension test). The S - N fatigue diagram (i.e., stress amplitude versus logarithm of the number of cycles to failure) for these alloys is shown in Figure 23.9.

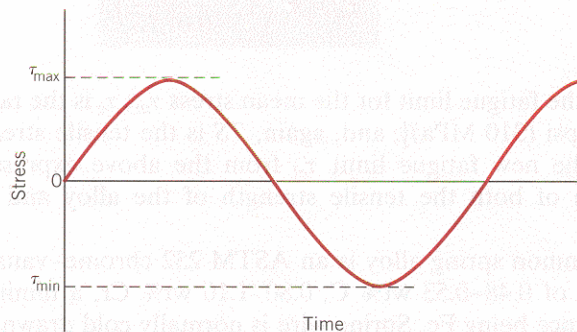


FIGURE 23.8 Stress versus time for a reversed cycle in shear.

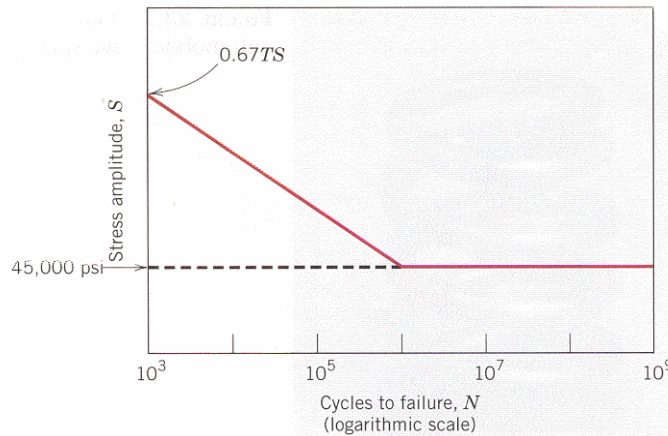


FIGURE 23.9 Shear stress amplitude versus logarithm of the number of cycles to fatigue failure for typical ferrous alloys.

Now let us estimate the number of cycles to which a typical valve spring may be subjected in order to determine whether it is permissible to operate within the fatigue limit regime of Figure 23.9 (i.e., if the number of cycles exceeds 10^6). For the sake of argument, assume that the automobile in which the spring is mounted travels a minimum of 100,000 miles (161,000 km) at an average speed of 40 mph (64.4 km/h), with an average engine speed of 3000 rpm (rev/min). The total time it takes the automobile to travel this distance is 2500 h (100,000 mi/40 mph), or 150,000 min. At 3000 rpm, the total number of revolutions is (3000 rev/min)(150,000 min) = 4.5×10^8 rev, and since there are 2 rev/cycle, the total number of cycles is 2.25×10^8 . This result means that we may use the fatigue limit as the design stress inasmuch as the limit cycle threshold has been exceeded for the 100,000-mile distance of travel (i.e., since 2.25×10^8 cycles $> 10^6$ cycles).

Furthermore, this problem is complicated by the fact that the stress cycle is not completely reversed (i.e., $\tau_m \neq 0$) inasmuch as between minimum and maximum deflections the spring remains in compression; thus, the 45,000 psi (310 MPa) fatigue limit is not valid. What we would now like to do is first to make an appropriate extrapolation of the fatigue limit for this $\tau_m \neq 0$ case and then compute and compare with this limit the actual stress amplitude for the spring; if the stress amplitude is significantly below the extrapolated limit, then the spring design is satisfactory.

A reasonable extrapolation of the fatigue limit for this $\tau_m \neq 0$ situation may be made using the following expression (termed Goodman's law):

$$\tau_{al} = \tau_e \left(1 - \frac{\tau_m}{0.67TS} \right) \quad (23.19)$$

where τ_{al} is the fatigue limit for the mean stress τ_m ; τ_e is the fatigue limit for $\tau_m = 0$ [i.e., 45,000 psi (310 MPa)]; and, again, TS is the tensile strength of the alloy. To determine the new fatigue limit τ_{al} from the above expression necessitates the computation of both the tensile strength of the alloy and the mean stress for the spring.

One common spring alloy is an ASTM 232 chrome–vanadium steel, having a composition of 0.48–0.53 wt% C, 0.80–1.10 wt% Cr, a minimum of 0.15 wt% V, and the balance being Fe. Spring wire is normally cold drawn (Section 12.2) to the desired diameter; consequently, tensile strength will increase with the amount of

drawing (i.e., with decreasing diameter). For this alloy it has been experimentally verified that, for the diameter d in inches, the tensile strength is

$$TS \text{ (psi)} = 169,000(d)^{-0.167} \quad (23.20)$$

Since $d = 0.170$ in. for this spring,

$$\begin{aligned} TS &= (169,000)(0.170 \text{ in.})^{-0.167} \\ &= 227,200 \text{ psi (1570 MPa)} \end{aligned}$$

Computation of the mean stress τ_m is made using Equation 8.21 modified to the shear stress situation as follows:

$$\tau_m = \frac{\tau_{\min} + \tau_{\max}}{2} \quad (23.21)$$

It now becomes necessary to determine the minimum and maximum shear stresses for the spring, using Equation 23.17. The value of τ_{\min} may be calculated from Equations 23.17 and 23.13 inasmuch as the minimum δ_c is known (i.e., $\delta_{ic} = 0.060$ in.). A shear modulus of 11.5×10^6 psi (79 GPa) will be assumed for the steel; this is the room-temperature value, which is also valid at the 80°C service temperature. Thus, τ_{\min} is just

$$\begin{aligned} \tau_{\min} &= \frac{\delta_{ic} G d}{\pi D^2} K_w \quad (23.22a) \\ &= \frac{\delta_{ic} G d}{\pi D^2} \left[1.60 \left(\frac{D}{d} \right)^{-0.140} \right] \\ &= \left[\frac{(0.060 \text{ in.})(11.5 \times 10^6 \text{ psi})(0.170 \text{ in.})}{\pi (1.062 \text{ in.})^2} \right] \left[1.60 \left(\frac{1.062 \text{ in.}}{0.170 \text{ in.}} \right)^{-0.140} \right] \\ &= 41,000 \text{ psi (280 MPa)} \end{aligned}$$

Now τ_{\max} may be determined taking $\delta_c = \delta_{mc} = 0.135$ in. as follows:

$$\begin{aligned} \tau_{\max} &= \frac{\delta_{mc} G d}{\pi D^2} \left[1.60 \left(\frac{D}{d} \right)^{-0.140} \right] \quad (23.22b) \\ &= \left[\frac{(0.135 \text{ in.})(11.5 \times 10^6 \text{ psi})(0.170 \text{ in.})}{\pi (1.062 \text{ in.})^2} \right] \left[1.60 \left(\frac{1.062 \text{ in.}}{0.170 \text{ in.}} \right)^{-0.140} \right] \\ &= 92,200 \text{ psi (635 MPa)} \end{aligned}$$

Now, from Equation 23.21,

$$\begin{aligned} \tau_m &= \frac{\tau_{\min} + \tau_{\max}}{2} \\ &= \frac{41,000 \text{ psi} + 92,200 \text{ psi}}{2} = 66,600 \text{ psi (460 MPa)} \end{aligned}$$

The variation of shear stress with time for this valve spring is noted in Figure 23.10; the time axis is not scaled, inasmuch as the time scale will depend on engine speed.

Our next objective is to determine the fatigue limit amplitude (τ_{al}) for this $\tau_m = 66,600$ psi (460 MPa) using Equation 23.19 and for τ_e and TS values of 45,000

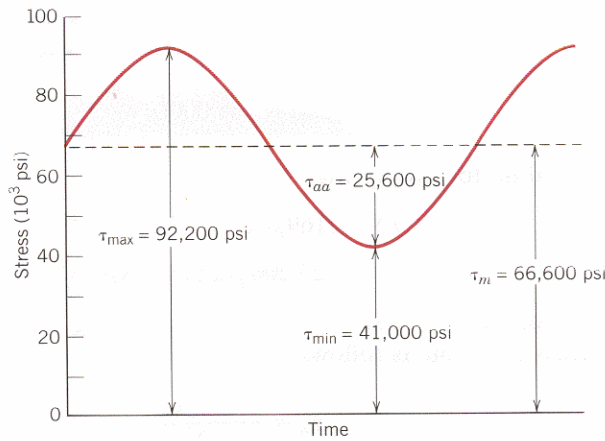


FIGURE 23.10 Shear stress versus time for an automobile valve spring.

psi (310 MPa) and 227,200 psi (1570 MPa), respectively. Thus,

$$\begin{aligned}\tau_{al} &= \tau_e \left[1 - \frac{\tau_m}{0.67TS} \right] \\ &= (45,000 \text{ psi}) \left[1 - \frac{66,600 \text{ psi}}{(0.67)(227,200 \text{ psi})} \right] \\ &= 25,300 \text{ psi (175 MPa)}\end{aligned}$$

Now let us determine the actual stress amplitude τ_{aa} for the valve spring using Equation 8.23 modified to the shear stress condition:

$$\begin{aligned}\tau_{aa} &= \frac{\tau_{\max} - \tau_{\min}}{2} \\ &= \frac{92,200 \text{ psi} - 41,000 \text{ psi}}{2} = 25,600 \text{ psi (177 MPa)}\end{aligned}\quad (23.23)$$

Thus, the actual stress amplitude is slightly greater than the fatigue limit, which means that this spring design is marginal.

The fatigue limit of this alloy may be increased to greater than 25,300 psi (175 MPa) by shot peening, a procedure described in Section 8.11. Shot peening involves the introduction of residual compressive surface stresses by plastically deforming outer surface regions; small and very hard particles are projected onto the surface at high velocities. This is an automated procedure commonly used to improve the fatigue resistance of valve springs; in fact, the spring shown in Figure 23.7 has been shot peened, which accounts for its rough surface texture. Shot peening has been observed to increase the fatigue limit of steel alloys in excess of 50% and, in addition, to reduce significantly the degree of scatter of fatigue data.

This spring design, including shot peening, may be satisfactory; however, its adequacy should be verified by experimental testing. The testing procedure is relatively complicated and, consequently, will not be discussed in detail. In essence, it involves performing a relatively large number of fatigue tests (on the order of 1000) on this shot-peened ASTM 232 steel, in shear, using a mean stress of 66,600 psi (460 MPa) and a stress amplitude of 25,600 psi (177 MPa), and for 10^6 cycles. On the basis of the number of failures, an estimate of the survival probability can be

made. For the sake of argument, let us assume that this probability turns out to be 0.99999; this means that one spring in 100,000 produced will fail.

Suppose that you are employed by one of the large automobile companies that manufactures on the order of 1 million cars per year, and that the engine powering each automobile is a six-cylinder one. Since for each cylinder there are two valves, and thus two valve springs, a total of 12 million springs would be produced every year. For the above survival probability rate, the total number of spring failures would be approximately 120, which also corresponds to 120 engine failures. As a practical matter, one would have to weigh the cost of replacing these 120 engines against the cost of a spring redesign.

Redesign options would involve taking measures to reduce the shear stresses on the spring, by altering the parameters in Equations 23.13 and 23.17. This would include either (1) increasing the coil diameter D , which would also necessitate increasing the wire diameter d , or (2) increasing the number of coils N_c .

ARTIFICIAL TOTAL HIP REPLACEMENT

23.6 ANATOMY OF THE HIP JOINT

As a prelude to discussing the artificial hip, let us first briefly address some of the anatomical features of joints in general and the hip joint in particular. The joint is an important component of the skeletal system. It is located at bone junctions, where loads may be transmitted from bone to bone by muscular action; this is normally accompanied by some relative motion of the component bones. Bone tissue is a complex natural composite consisting of soft and strong protein collagen and brittle apatite, which has a density between 1.6 and 1.7 g/cm³. Being an anisotropic material, the mechanical properties of bone differ in longitudinal (axial) and transverse (radial) directions (Table 23.3). The articulating (or connecting) surface of each joint is coated with cartilage, which consists of body fluids that lubricate and provide an interface having a very low coefficient of friction so as to facilitate the bone-sliding movement.

The human hip joint (Figure 23.11) occurs at the junction between the pelvis and the upper leg (thigh) bone, or femur. A relatively large range of rotary motion is permitted at the hip by a ball-and-socket type of joint; the top of the femur

Table 23.3 Mechanical Characteristics of Human Long Bone Both Parallel and Perpendicular to the Bone Axis

<i>Property</i>	<i>Parallel to Bone Axis</i>	<i>Perpendicular to Bone Axis</i>
Elastic modulus, GPa (psi)	17.4 (2.48×10^6)	11.7 (1.67×10^6)
Ultimate strength, tension, MPa (ksi)	135 (19.3)	61.8 (8.96)
Ultimate strength, compression, MPa (ksi)	196 (28.0)	135 (19.3)
Elongation at fracture	3–4%	—

Source: From D. F. Gibbons, “Biomedical Materials,” pp. 253–254, in *Handbook of Engineering in Medicine and Biology*, D. G. Fleming, and B. N. Feinberg, CRC Press, Boca Raton, Florida, 1976. With permission.

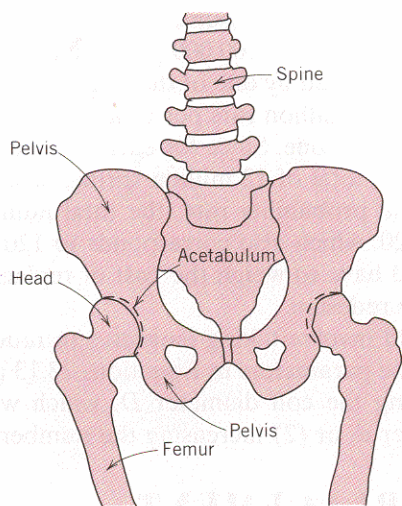


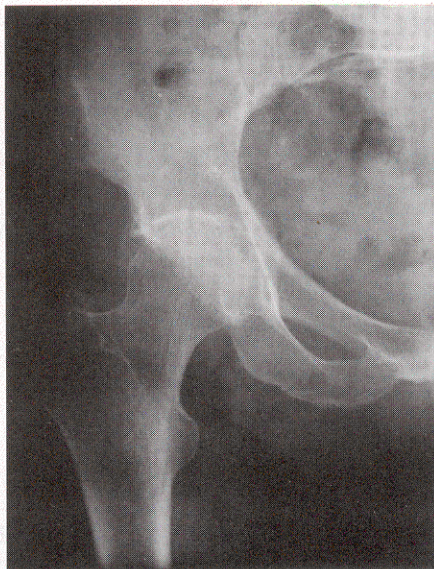
FIGURE 23.11 Schematic diagram of human hip joints and adjacent skeletal components.

terminates in a ball-shaped head that fits into a cuplike cavity (the acetabulum) within the pelvis. An x-ray of a normal hip joint is shown in Figure 23.12a.

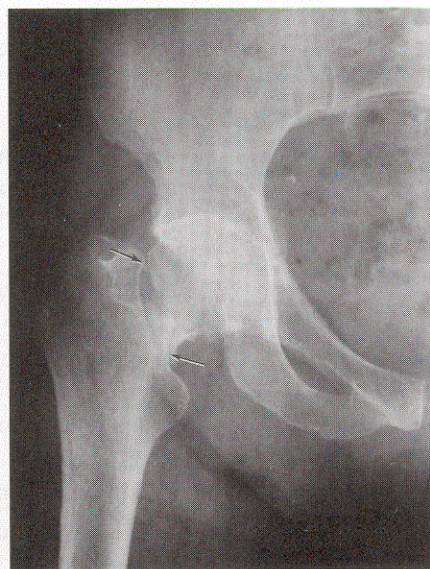
This joint is susceptible to fracture, which normally occurs at the narrow region just below the head. An x-ray of a fractured hip is shown in Figure 23.12b; the arrows show the two ends of the fracture line through the femoral neck. Furthermore, the hip may become diseased (osteoarthritis); in such a case small lumps of bone form on the rubbing surfaces of the joint, which causes pain as the head rotates in the acetabulum. Damaged and diseased hip joints have been replaced with artificial or prosthetic ones, with moderate success, beginning in the late 1950s. Total hip replacement surgery involves the removal of the head and the upper portion of the femur, and some of the bone marrow at the top of the remaining femur segment. Into this hole within the center of the femur is secured a metal anchorage stem

FIGURE 23.12

X-Rays of (a) a normal hip joint and (b) a fractured hip joint. The arrows in (b) show the two ends of the fracture line through the femoral neck.

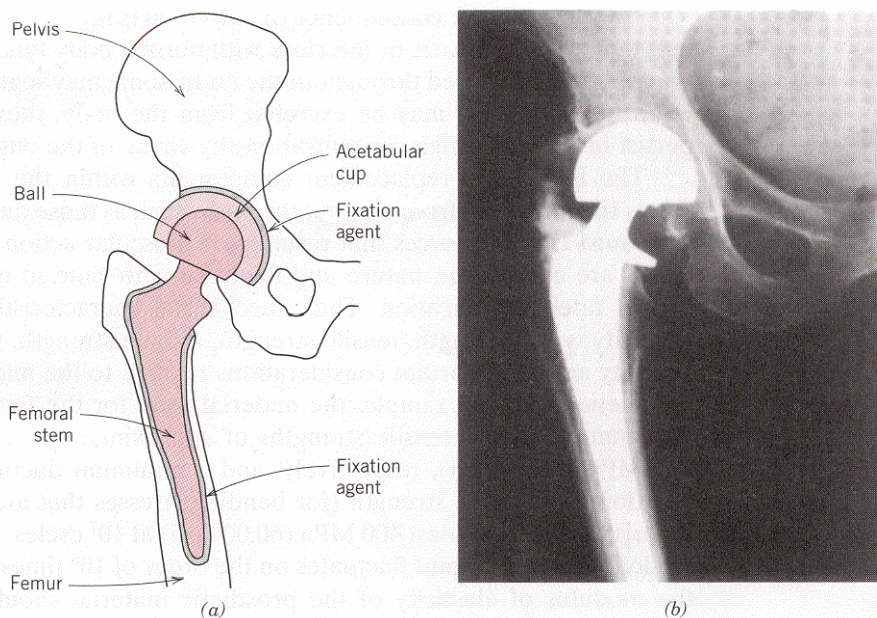


(a)



(b)

FIGURE 23.13
(a) Schematic diagram and (b) x-ray of an artificial total hip replacement.



onto which is attached, at its other end, the ball portion of the joint. In addition, the replacement cup socket must be attached to the pelvis. This is accomplished by removal of the old cup and its surrounding bone tissue. The new socket is affixed into this recess. A schematic diagram of the artificial hip joint is presented in Figure 23.13a; and Figure 23.13b shows an x-ray of a total hip replacement. In the remainder of this section we discuss material constraints and those materials that have been used with the greatest degree of success for the various artificial hip components.

23.7 MATERIAL REQUIREMENTS

In essence, there are four basic components to the artificial hip: (1) the femoral stem, (2) the ball that attaches to this stem, (3) the acetabular cup that is affixed to the pelvis, and (4) a fixation agent that secures the stem into the femur and the cup to the pelvis. The property constraints on the materials to be used for these elements are very stringent because of the chemical and mechanical complexity of the hip joint. Some of the requisite material characteristics will now be discussed.

Whenever any foreign material is introduced into the body environment, rejection reactions occur. The magnitude of rejection may range from mild irritation or inflammation to death. Any implant material must be *biocompatible*, that is, it must produce a minimum degree of rejection. Products resulting from reactions with body fluids must be tolerated by the surrounding body tissues such that normal tissue function is unimpaired. Biocompatibility is a function of the location of the implant, as well as of its chemistry and shape.

The body fluid consists of an aerated and warm solution containing approximately 1 wt% NaCl in addition to other salts and organic compounds in relatively minor concentrations. Thus, the body fluids are very corrosive, which, for metal alloys can lead not only to uniform corrosion, but also to crevice attack and pitting and, when stresses are present, to fretting, stress corrosion cracking, and corrosion fatigue. It has been estimated that the maximum tolerable corrosion rate for implant metal alloys is on the order of 0.01 mil per year (2.5×10^{-4} mm per year).

Another adverse consequence of corrosion is the generation of corrosion products that are either toxic or interfere with normal body functions. These substances are rapidly transported throughout the body; some may segregate in specific organs. Even though others may be excreted from the body, they may nevertheless still persist in relatively high concentrations by virtue of the ongoing corrosion process.

The bones and replacement components within the hip joint must support forces that originate from without the body, such as those due to gravity; in addition, they must transmit forces that result from muscular action such as walking. These forces are complex in nature and fluctuate with time in magnitude, in direction, and in rate of application. Thus, mechanical characteristics such as modulus of elasticity, yield strength, tensile strength, fatigue strength, fracture toughness, and ductility are all important considerations relative to the materials of choice for the prosthetic hip. For example, the material used for the femoral stem should have minimum yield and tensile strengths of approximately 500 MPa (72,500 psi) and 650 MPa (95,000 psi), respectively, and a minimum ductility of about 8%EL. In addition, the fatigue strength (for bending stresses that are fully reversed [Figure 8.20a]) should be at least 400 MPa (60,000 psi) at 10^7 cycles. For the average person, the load on the hip joint fluctuates on the order of 10^6 times per year. Furthermore, the modulus of elasticity of the prosthetic material should match that of bone; a significant difference can lead to deterioration of the bone tissue surrounding the implant.

Furthermore, since the ball-and-cup articulating surfaces rub against one another, wear of these surfaces is minimized by the employment of very hard materials. Excessive and uneven wear can lead to a change in shape of the articulating surfaces and cause the prosthesis to malfunction. In addition, particulate debris will be generated as the articulating surfaces wear against one another; accumulation of this debris in the surrounding tissues can also lead to inflammation.

Frictional forces at these rubbing counterfaces should also be minimized to prevent loosening of the femoral stem and acetabular cup assembly from their positions secured by the fixation agent. If these components do become loose over time, the hip will experience premature degradation that may require it to be replaced.

Three final important material factors are density, property reproducibility, and cost. It is highly desirable that lightweight components be used, that material properties from prosthesis to prosthesis remain consistent over time, and, of course, that the cost of the prosthesis components be reasonable.

Ideally, an artificial hip that has been surgically implanted should function satisfactorily for the lifetime of the recipient and not require replacement. For current designs, lifetimes range between only five and ten years; certainly longer ones are desirable.

Several final comments are in order relative to biocompatibility assessment. Biocompatibility of materials is usually determined empirically; that is, tests are conducted wherein materials are implanted in laboratory animals and the biocompatibility of each material is judged on the basis of rejection reactions, level of corrosion, generation of toxic substances, etc. This procedure is then repeated on humans for those materials that were found to be relatively biocompatible in animals. It is difficult to *a priori* predict the biocompatibility of a material. For example, mercury, when ingested into the body, is poisonous; however, dental amalgams, which have high mercury contents, have generally been found to be very biocompatible.

23.8 MATERIALS EMPLOYED

FEMORAL STEM AND BALL

Early prosthetic hip designs called for both the femoral stem and ball to be of the same material—a stainless steel. Subsequent improvements have been introduced, including the utilization of materials other than stainless steel and, in addition, constructing the stem and ball from different materials. Figure 23.14 is a photograph in which are shown two different hip replacement designs.

Currently, the femoral stem is constructed from a metal alloy of which there are three possible types: stainless steel, cobalt–nickel–chromium–molybdenum, and titanium. The most suitable stainless steel is 316L, which has a very low sulfur content (<0.002 wt%); its composition is given in Table 12.4. The principal disadvantages of this alloy are its susceptibility to crevice corrosion and pitting, and its relatively low fatigue strength. Fabrication technique may also have a significant influence on its characteristics. Cast 316L typically has poor mechanical properties and inadequate corrosion resistance. Consequently, prosthetic femoral stems are either forged or cold worked. Furthermore, heat treatment may also influence the characteristics of the material and must be taken into consideration. Normally, 316L is implanted in older and less active persons. The mechanical characteristics and corrosion rate range of this alloy (in the cold-worked state) are supplied in Table 23.4.

Various Co–Cr–Mo and Co–Ni–Cr–Mo alloys have been employed for artificial hip prostheses; one that has been found to be especially suitable, designated MP35N, has a composition of 35 wt% Co, 35 wt% Ni, 20 wt% Cr, and 10 wt% Mo. It is formed by hot forging and, as such, has tensile and yield strengths that are superior to 316L stainless steel (Table 23.4). Furthermore, its corrosion and fatigue characteristics are excellent.

Of those metal alloys that are implanted for prosthetic hip joints, probably the most biocompatible is the titanium alloy Ti–6Al–4V; its composition is 90 wt% Ti, 6 wt% Al, and 4 wt% V. The optimal properties for this material are produced by hot forging; any subsequent deformation and/or heat treatment should be avoided to prevent the formation of microstructures that are deleterious to its bioperformance. The properties of this alloy are also listed in Table 23.4.

Recent improvements for this prosthetic device include using a ceramic material for the ball component rather than any of the aforementioned metal alloys. The ceramic of choice is a high-purity and polycrystalline aluminum oxide, which is

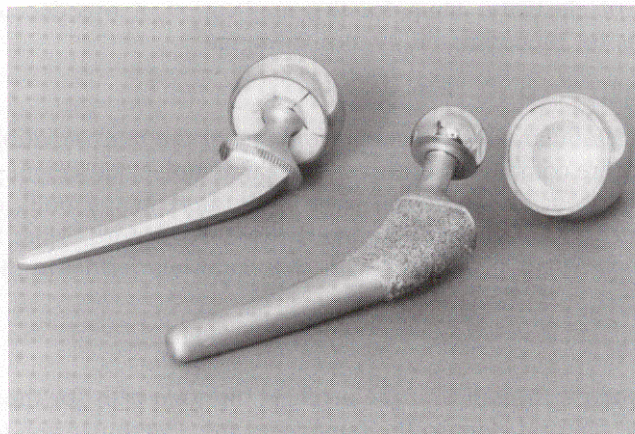


FIGURE 23.14 Photograph showing two artificial total hip replacement designs.

Table 23.4 Mechanical and Corrosion Characteristics of Three Metal Alloys That Are Commonly Used for the Femoral Stem Component of the Prosthetic Hip

<i>Alloy</i>	<i>Elastic Modulus [GPa (psi)]</i>	<i>0.2% Yield Strength [MPa (ksi)]</i>	<i>Tensile Strength [MPa (ksi)]</i>	<i>Elongation at Fracture (%)</i>	<i>Fatigue Strength or Limit, 10⁷ Cycles [MPa (ksi)]</i>	<i>Corrosion Rate (mpy)^a</i>
316L Stainless steel (cold worked)	196 (28.4 × 10 ⁶)	700 (102)	875 (127)	12	383 (55.5)	0.001–0.002
MP35N (hot forged)	230 (33.4 × 10 ⁶)	1000 (145)	1200 (174)	13	500 (72.5)	0.0012–0.002
Ti-6Al-4V (hot forged)	120 (17.4 × 10 ⁶)	950 (138)	1075 (156)	13	580 (84.1)	0.007–0.04

^a mpy means mils per year, or 0.001 in./yr

Sources: From Gladius Lewis, *Selection of Engineering Materials*, © 1990, p. 189. Adapted by permission of Prentice Hall, Englewood Cliffs, New Jersey. And D. F. Gibbons, “Materials for Orthopedic Joint Prostheses,” Ch. 4, p. 116, in *Biocompatibility of Orthopedic Implants*, Vol. I, D. F. Williams, CRC Press, Boca Raton, Florida, 1982. With permission.

harder and more wear resistant, and generates lower frictional stresses at the joint. However, the fracture toughness of alumina is relatively low and its fatigue characteristics are poor. Hence, the femoral stem, being subjected to significant stress levels, is still fabricated from one of the above alloys, and is then attached to the ceramic ball; this femoral stem–ball component thus becomes a two-piece unit.

The materials selected for use in an orthopedic implant come after years of research into the chemical and physical properties of a host of different candidate materials. Ideally, the material(s) of choice will not only be biocompatible, but have mechanical properties that match the biomaterial being replaced—viz., bone. However, no man-made material is both biocompatible and possesses the property combination of bone and the natural hip joint—i.e., low modulus of elasticity, relatively high strength and fracture toughness, low coefficient of friction, and excellent wear resistance. Consequently, material property compromises and trade-offs must be made. For example, recall that the modulus of elasticity of bone and femoral stem materials should be closely matched such that accelerated deterioration of the bone tissue adjacent to the implant is avoided. Unfortunately, man-made materials that are both biocompatible and relatively strong, also have high moduli of elasticity. Thus, for this application, it was decided to trade off a low modulus for biocompatibility and strength.

ACETABULAR CUP

Some acetabular cups are made from one of the biocompatible alloys or aluminum oxide. More commonly, however, ultrahigh molecular weight polyethylene (Section 16.18) is used. This material is virtually inert in the body environment and has excellent wear-resistance characteristics; furthermore, it has a very low coefficient of friction when in contact with the materials used for the ball component of the socket.

FIXATION

Successful performance of the artificial hip joint calls for the secure attachment of both the femoral stem to the femur and the acetabular cup to the pelvis. Insecure attachment of either component ultimately leads to a loosening of that component

and the accelerated degradation of the joint. A fixation agent is sometimes used to bond these two prosthetic components to their surrounding bone structures. The most commonly used fixation agent is a polymethyl methacrylate (acrylic) bone cement that is polymerized *in situ* during surgery.

This acrylic bond cement has, in some cases, contributed to femoral stem loosening because it is brittle and does not bond well with the metallic implant and bone tissue. It has been found that a more secure implant–bone bond is formed when the stem is coated with a porous surface layer, consisting of a sintered metal powder. After implantation, bone tissue grows into the three-dimensional pore network, and thereby fixates the implant to the bone. Such a coating has been applied to the upper stem region of the right hip replacement shown in Figure 23.14.

THERMAL PROTECTION SYSTEM ON THE SPACE SHUTTLE ORBITER

23.9 INTRODUCTION

In 1969, the National Aeronautics and Space Administration (NASA) of the United States decided to direct its primary mission to the development of a *Space Transportation System (STS)*, also commonly known as the *Space Shuttle Orbiter*. In essence, the Space Shuttle is a reusable cargo-carrying space vehicle that is launched aboard a rocket, and then orbits the earth. Upon mission completion, it reenters the atmosphere as a space craft, and, finally, once inside the lower atmosphere, lands in the manner of a normal aircraft. The maiden flight was made by the *Columbia* orbiter in April of 1981; since then, four other orbiters have been constructed—*Discovery*, *Atlantis*, *Endeavour*, and the ill-fated *Challenger*. A photograph of the *Atlantis* is shown on page 734.

The successful operation of the Space Shuttle is dependent on a fully reusable outer “skin,” termed a *Thermal Protection System (TPS)*, that protects the inner airframe and its occupants from the searing heat generated during the reentry phase from space into the earth’s atmosphere. The development of this Thermal Protection System evolved over a twenty-year period, and is a classical and somewhat involved materials selection and design problem. In this section the primary components of the Shuttle’s TPS are discussed.

In reading this section, keep in mind that cost constraints relative to the design and fabrication of these materials were not as rigid as would be expected for normal commercial applications.

23.10 THERMAL PROTECTION SYSTEM— DESIGN REQUIREMENTS

Material requirements on the Thermal Protection System are, to say the least, awesome. For example, the TPS must do the following:

1. Maintain the temperature on the inner airframe below that to which it was designed [viz., 175°C (350°F)] for a maximum outer surface temperature of 1260°C (2300°F).
2. Remain usable for 100 missions, with a maximum turnaround time of 160 h.
3. Provide and maintain an aerodynamically smooth outer surface.

4. Be constructed of low-density materials.
5. Withstand temperature extremes between -110°C (-170°F) and 1260°C (2300°F).
6. Be resistant to severe thermal gradients and rapid temperature changes.
7. Be able to withstand stresses and vibrations that are experienced during launch, as well as thermally induced stresses imposed during temperature changes.
8. Experience a minimum absorption of moisture and other contaminants during storage between missions.
9. Be made to adhere to the airframe that is constructed of an aluminum alloy.

Thermal protection systems and materials developed previously by the aerospace industry proved unsuitable for the Space Shuttle because they were either too dense and/or nonreusable. Therefore, it became necessary to design a new set of complex materials. Furthermore, no single material is capable of meeting all of the criteria listed above. In addition, not all of these criteria are required over all surfaces of the spacecraft; for example, typical reentry maximum temperature profiles are shown in Figure 23.15.

Therefore, the philosophy adopted was to design several different thermal protection materials systems, each with its particular set of properties, that satisfy the required criteria for a specific region of the spacecraft surface. Several different materials systems are employed on the Space Shuttles, the designs of which depend

FIGURE 23.15

Approximate maximum outer surface temperature profiles for the Space Shuttle

Orbiter during reentry:

(a) upper and lower views; (b) side view.

(From "The Shuttle Orbiter Thermal Protection System,"

L. J. Korb, C. A. Morant,

R. M. Calland, and

C. S. Thatcher, *Ceramic*

Bulletin, No. 11, Nov.

1981, p. 1188.

Copyright 1981.

Reprinted by

permission of the

American Ceramic

Society.)

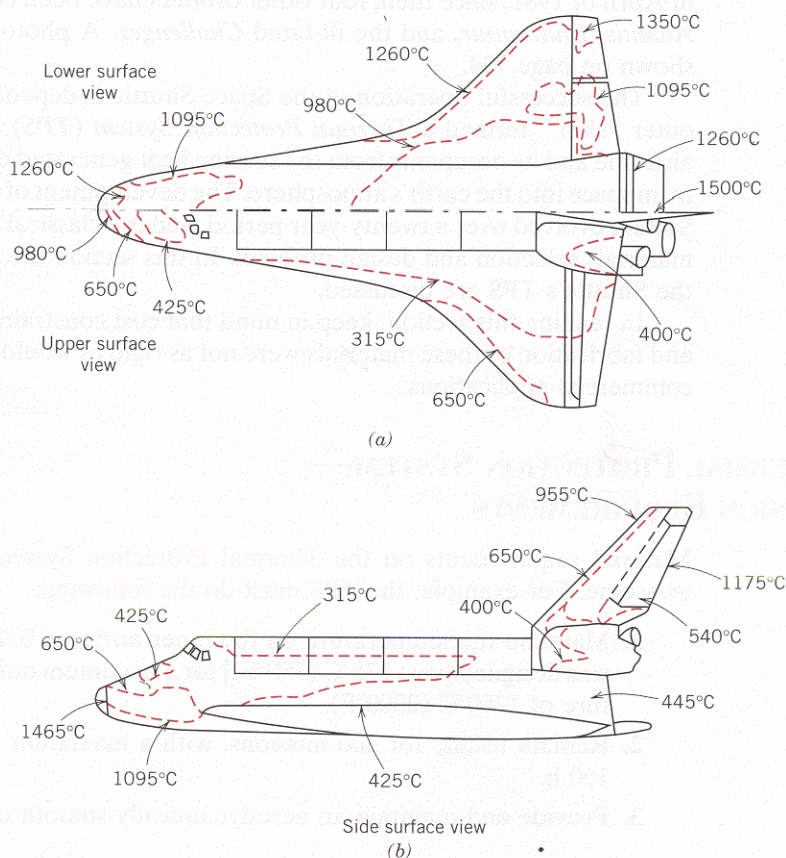


Table 23.5 Thermal Protection Systems Employed on the Space Shuttle Orbiter

<i>Material Generic Name</i>	<i>Minimum Operating Temperature, °C (°F)</i>	<i>Maximum Operating Temperature, °C (°F)</i>	<i>Material Composition</i>	<i>Orbiter Locations</i>
Felt reusable surface insulation (FRSI)	−130 (−200)	400 (750)	Nylon felt, silicone rubber coating	Wing upper surface, upper sides, cargo bay doors
Advanced flexible reusable surface insulation (AFRSI)	−130 (−200)	815 (1500)	Quartz batting sandwiched between quartz and glass fabrics	Upper surface regions
Low-temperature reusable surface insulation (LRSI)	−130 (−200)	650 (1200)	Silica tiles, borosilicate glass coating	Upper wing surfaces, tail surfaces, upper vehicle sides
High-temperature reusable insulation (HRSI)	−130 (−200)	1260 (2300)	Silica tiles, borosilicate glass coating with SiB ₄ added	Lower surfaces and sides, tail leading and trailing edges
Reinforced carbon–carbon (RCC)	No lower limit identified	1650 (3000)	Pyrolyzed carbon–carbon, coated with SiC	Nose cap and wing leading edges

Source: Adapted from L. J. Korb, C. A. Morant, R. M. Calland and C. S. Thatcher, “The Shuttle Orbiter Thermal Protection System,” *Ceramic Bulletin*, No. 11, Nov. 1981, p. 1188. Copyright 1981. Reprinted by permission of the American Ceramic Society.

on the maximum outer surface temperature generated during vehicle reentry. These systems and their temperature ranges of operation, material compositions, and orbiter areas are listed in Table 23.5. Furthermore, the locations of these various systems are indicated in Figure 23.16.

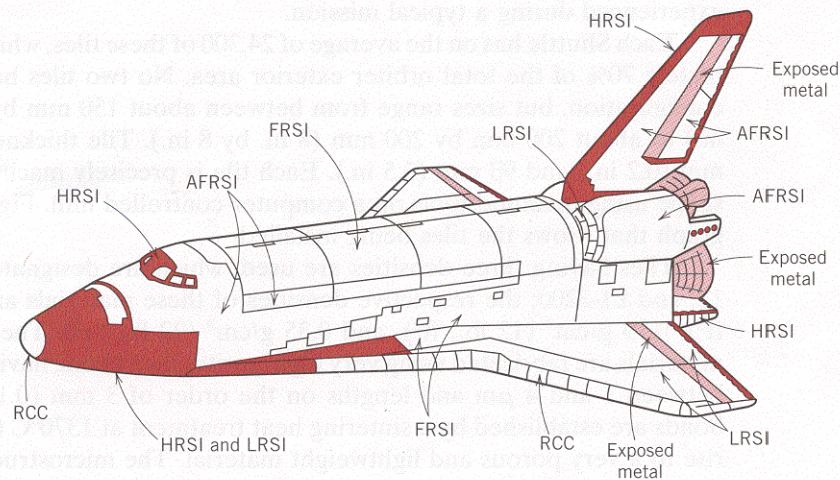


FIGURE 23.16 Locations of the various components of the thermal protection system on the Space Shuttle Orbiter: FRSI, felt reusable surface insulation; AFRSI, advanced flexible reusable surface insulation; LRSI, low-temperature reusable surface insulation; HRSI, high-temperature reusable surface insulation; RCC, reinforced carbon–carbon composite. (Adapted from L. J. Korb, C. A. Morant, R. M. Calland, and C. S. Thatcher, “The Shuttle Orbiter Thermal Protection System,” *Ceramic Bulletin*, No. 11, Nov. 1981, p. 1189. Copyright 1981. Reprinted by permission of the American Ceramic Society.)

23.11 THERMAL PROTECTION SYSTEM—COMPONENTS

FELT REUSABLE SURFACE INSULATION

Upper surface regions exposed up to temperatures of 400°C (750°F) are covered with what is termed *felt reusable surface insulation (FRSI)*. This insulation consists of felt blankets of a nylon material the outer surface of which is coated with a silicone elastomer to achieve the necessary surface thermal properties. These blankets come in two thicknesses, 4 and 8 mm (0.16 and 0.32 in.), and are bonded to the aluminum airframe by a room-temperature vulcanizing (RTV) silicone adhesive.

Other upper surface regions that are exposed to higher temperatures, not to exceed 815°C (1500°F), are protected by blankets of an *advanced flexible reusable surface insulation (AFRSI)*. These blankets consist of a quartz fiber batting that is sandwiched between a high-temperature woven quartz fabric on the outer side and a lower-temperature glass fabric on the inner side. The outer surface of some regions is also protected with a ceramic coating. Furthermore, these three layers are stitched together using quartz and glass threads in a one-inch square pattern. AFRSI blanket thicknesses range between 10 mm (0.41 in.) and just under 50 mm (2 in.). Over most vehicle regions, these AFRSI blankets are bonded to the structure by a silicone RTV adhesive, as with the FRSI insulation.

CERAMIC TILE SYSTEMS

More rigid material restrictions are imposed on regions of the Space Shuttle that are exposed to temperatures in the range of 400 to 1260°C (750 to 2300°F). For these areas it was decided to use a relatively complex ceramic material in the form of tiles. Ceramics are intrinsically thermal insulators and, furthermore, will withstand these elevated temperatures. The tile design is utilized for the protection system to conform to the contours of the Shuttle's surface, and also to accommodate the thermal dimensional changes accompanying the extremes of temperature that are experienced during a typical mission.

Each Shuttle has on the average of 24,300 of these tiles, which comprise approximately 70% of the total orbiter exterior area. No two tiles have exactly the same configuration, but sizes range from between about 150 mm by 150 mm (6 in. by 6 in.) to about 200 mm by 200 mm (8 in. by 8 in.). Tile thicknesses vary between 5 mm (0.2 in.) and 90 mm (3.5 in.). Each tile is precisely machined to its individual shape using diamond tools on a computer-controlled mill. Figure 23.17 is a photograph that shows the tiles being installed.

Tiles having three densities are used, which are designated by LI-900, FRCI-12, and LI-2200; the respective densities of these materials are 0.14 g/cm³ (9 lb_m/ft³), 0.19 g/cm³ (12 lb_m/ft³), and 0.35 g/cm³ (22 lb_m/ft³). The LI-900 and LI-2200 materials are fabricated using very high-purity silica fibers, having diameters ranging between 1 and 4 μm and lengths on the order of 3 mm (0.13 in.). Fiber-to-fiber bonds are established by a sintering heat treatment at 1370°C (2500°F), which gives rise to a very porous and lightweight material. The microstructure of a typical tile is shown in the scanning electron micrograph, Figure 23.18. On the other hand, FRCI tiles are composed of a 78% silica fiber-22% aluminum borosilicate fiber composite; the FRCI designation comes from *Fibrous Refractory Composite Insulation*.

The strengths of the LI-2200 and FRCI tiles are virtually equivalent, being greater than that of LI-900. LI-2200 and FRCI are used in those locations where a higher strength is required, such as around doors and access panels. Employment

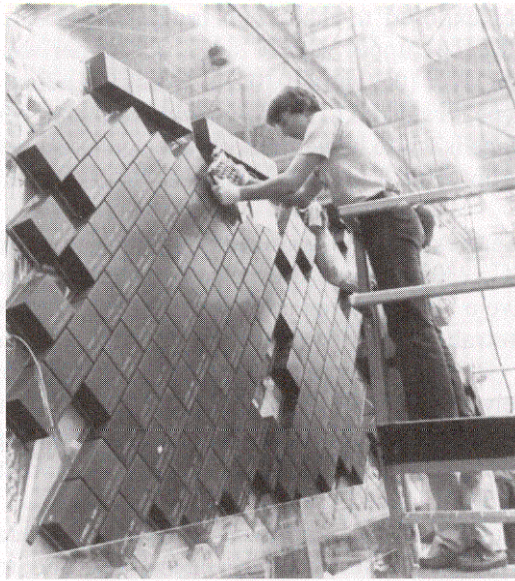


FIGURE 23.17 Photograph showing the installation of thermal protection ceramic tiles on the Space Shuttle Orbiter. [Photograph courtesy the National Aeronautics and Space Administration (NASA).]

of FRCI instead of LI-2200 reduced orbiter weight by approximately 450 kg (1000 lb_m). Most tiles on the orbiters are the LI-900 type.

These low-density silica fiber materials are ideal for the Shuttle's Thermal Protection System. Being approximately 93 vol% void, they are excellent thermal insulators; this is confirmed by the photograph on page 658, which shows a man holding a very hot cube of the tile material in his bare hands. Furthermore, silica has an extremely low coefficient of thermal expansion (Table 20.1) as well as a relatively small modulus of elasticity (Table 13.5); thus, it is very resistant to thermal shock associated with rapid temperature changes (Equation 20.8). Also, silica may be heated to relatively high temperatures without softening; short-term exposures to temperatures as high as 1480°C (2700°F) are possible.

The properties of the tiles are anisotropic; they are designed to be strongest in the plane of the tile and to be most thermally insulative in the direction perpendicular to this plane.

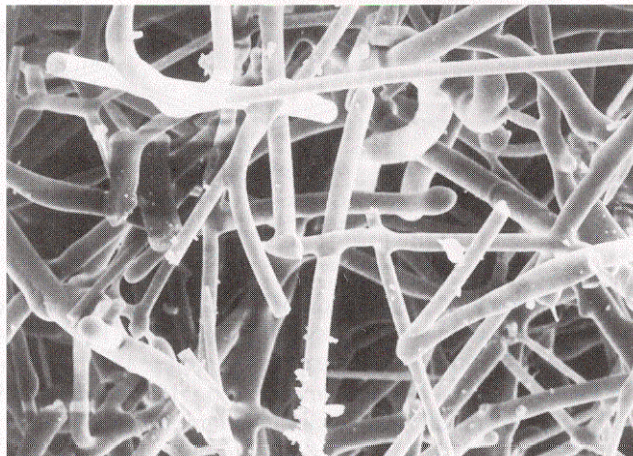


FIGURE 23.18 Scanning electron micrograph of a Space Shuttle Orbiter ceramic tile showing silica fibers that were bonded to one another during a sintering heat treatment. 750×. (Photograph provided courtesy of Lockheed Aerospace Ceramics Systems, Sunnyvale, California.)

Tiles on surfaces exposed to maximum temperatures in the range of 400 to 650°C (750 to 1200°F) (i.e., upper vehicle sides, and upper wing and tail surfaces) are coated with a thin layer (0.30 mm [0.012 in.] thick) of a high-emittance borosilicate glass. This tile type is referred to as a *low-temperature reusable surface insulation (LRSI)*; the tile surface is white, which reflects the sun's rays and keeps the Shuttle relatively cool while in orbit. Locations of the LRSI tiles are indicated in Figure 23.16.

Those tiles that are exposed to higher maximum temperatures between 650°C (1200°F) and 1260°C (2300°F) (i.e., the vehicle underbody, and tail leading and trailing edges) receive a black coating consisting of the same borosilicate glass and, in addition, silicon tetraboride (SiB_4); this coating material is sometimes termed a *reaction cured glass (RCG)*. Being of high optical emittance, this coating is able to radiate approximately 90% of the reentry heat generated away from the Shuttle either into the earth's atmosphere or into deep space. This type of tile is termed a *high-temperature reusable surface insulation (HRSI)*, and its locations on the Shuttle are also noted in Figure 23.16.

It is also necessary to isolate and cushion the brittle ceramic tiles from the mechanical and thermal strains sustained by the airframe and, in addition, to attach the tiles to the airframe. This is accomplished by an assembly consisting of a *strain isolator pad (SIP)*, a *filler bar*, and a silicone RTV adhesive that bonds the tile to the SIP and the SIP and filler bar to the airframe structure. A schematic diagram of this assembly is shown in Figure 23.19. The strain isolator pad is composed of a nylon felt that will sustain repeated heatings to 290°C (550°F); this pad isolates the tiles from airframe deflections.

Beneath the tile-to-tile junctions are located the filler bars. They are of the same nylon felt to which an RTV outer coating has been applied. The thickness of these bars is greater than the strain isolator pad, and, as such, they form a gasket seal to the undersurface of the tiles and protect the strain isolator pads from water or plasma penetration through the tile-to-tile junctions.

The adhesive that bonds this system together and to the airframe must survive repeated exposures to at least 290°C (550°F), must cure at room temperature, and

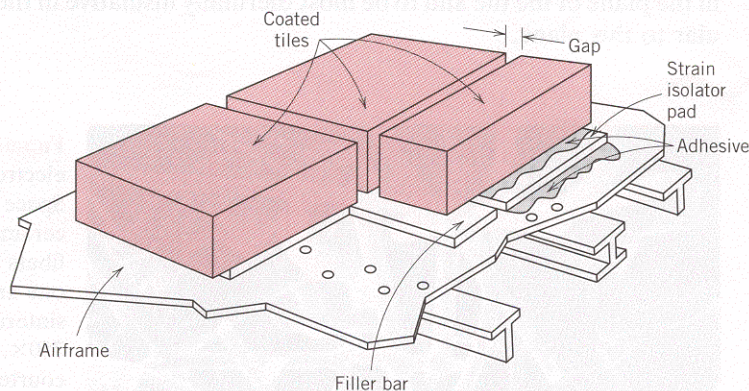


FIGURE 23.19 Schematic cross section of the tile component of the Space Shuttle Orbiter's thermal protection system. (From L. J. Korb, C. A. Morant, R. M. Calland, and C. S. Thatcher, "The Shuttle Orbiter Thermal Protection System," *Ceramic Bulletin*, No. 11, Nov. 1981, p. 1189. Copyright 1981. Reprinted by permission of the American Ceramic Society.)

must be capable of filling any irregularities in the airframe structure. The only material that fulfills all these requirements is a silicone RTV adhesive.

REINFORCED CARBON–CARBON

During reentry, some shuttle orbiter surface regions are exposed to temperatures in excess of those that the ceramic tiles are capable of sustaining (1260°C [2300°F]). Specifically, these areas are the nose cap and wing leading edges, Figure 23.15, where temperatures may reach as high as 1650°C (3000°F). The material that was designed for use in these locations is a *reinforced carbon–carbon* (RCC) composite. It is also a relatively complex material consisting of a carbon matrix that is reinforced with graphite fibers; the surface is coated with a thin layer of silicon carbide (SiC) as a protection against oxidation. This composite material is suitable for these high-temperature locations for the following reasons: strength and stiffness are retained up to the maximum service temperatures; it has a low coefficient of thermal expansion, and thus will not experience significant thermal stresses and deflections; it is highly resistant to thermal shock and fatigue; its density is very low; and fabrication into complex shapes is possible. Figure 23.16 shows those areas where this RCC composite material is employed.

Of course, materials other than those already cited are used on the Orbiter. For example, window ports are made of glass materials. Also, as may be noted from Figure 23.16, metal alloys are used for some exposed surfaces. These alloys will typically have high melting temperatures and, preferably, relatively low densities. Examples include beryllium, niobium, titanium, stainless steel (alloys 316), and several superalloys (Inconel alloys 718, 625, 750, and Haynes alloy 188).

MATERIALS FOR INTEGRATED CIRCUIT PACKAGES

23.12 INTRODUCTION

The microelectronic circuitry, including the integrated circuits that are used in our modern computers, calculators, and other electronic devices, was briefly discussed in Section 19.14. The heart of the integrated circuit (abbreviated *IC*) is the *chip*, a small rectangular substrate of high-purity and single-crystal silicon (or more recently gallium arsenide) onto which literally thousands of circuit elements are imprinted. Circuit elements (i.e., transistors, resistors, diodes, etc.) are created by selectively adding controlled concentrations of specific impurities to extremely minute and localized regions near the surface of the semiconducting material using involved photolithographic techniques. The chips are small in size, with the largest being on the order of 6 mm ($\frac{1}{4}$ in.) on each side and approximately 0.4 mm (0.015 in.) thick. Photographs of a typical chip are shown in Figure 19.25.

Furthermore, chips are very fragile inasmuch as silicon is a relatively brittle material and gallium arsenide is even more brittle. It is also necessary to fabricate conducting circuit paths over the surface of the chip so as to facilitate the passage of current from device to device; on silicon ICs the metal conductor used is aluminum or an aluminum–silicon alloy (99 wt% Al, 1 wt% Si) which is metallized onto the chip surface to form a very thin film. The chip design also calls for these circuit paths to terminate at contact pads on the chip periphery, at which points electrical

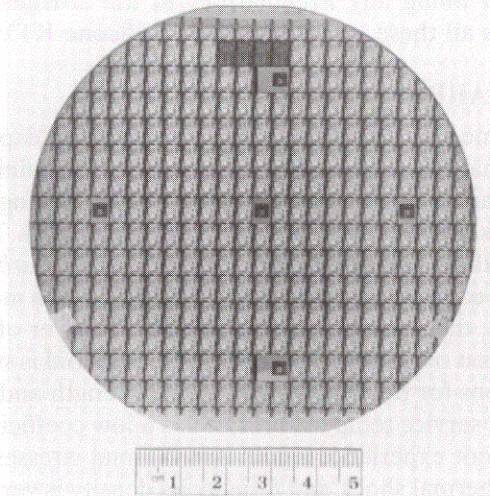


FIGURE 23.20 Photograph of a 100-mm-diameter (4-in.-diameter) silicon wafer. Each of the small rectangles shown is an individual IC chip or die.

connections may be made with the macroscopic world. It should be obvious that a functioning microelectronic chip is a very sophisticated electronic entity, that materials requirements are very stringent, and that elegant processing techniques are involved in its fabrication.

A large number of IC chips are fabricated onto a circular thin wafer of single-crystal Si, as shown in the photograph in Figure 23.20. Single crystals of Si having diameters as large as 200 mm (8 in.) are routinely grown. The small rectangular ICs arrayed in the manner shown in the photograph are collectively referred to as *dice*. Each IC or *die* (singular of dice) is first tested for functionality, after which it is removed from the wafer in a meticulous sawing or “scribe and break” operation. Next, the die is mounted in some type of *package*. The packaged IC may then be bonded to a printed circuit board. The purpose of this section is to discuss the material requirements and some of the materials that are used for the various IC package components.

Some of the functions that an integrated circuit package must perform include the following:

1. To permit electrical contact between the devices on the chip and the macroscopic world. The contact pads on the surface of the IC are so minuscule and numerous that accommodation of macroscopic wiring is simply not possible.
2. To dissipate excess heat. While in operation, the many electronic devices generate significant quantities of heat, which must be dissipated away from the chip.
3. To protect delicate electrical connections on the chip from chemical degradation and contamination.
4. To provide mechanical support so that the small and fragile chip may be handled.
5. To provide an adequate electrical interface such that the performance of the IC itself is not significantly degraded by the package design.

Thus, IC packaging also poses a host of material demands that are very challenging. In fact, it has been noted that the performance of some ICs is limited, not by

the characteristics of the semiconducting materials nor by the metallization process, but rather by the quality of the package. There are a number of different package designs used by the various IC manufacturers. For one of the common designs, the *leadframe*, we have elected to discuss the various components and, for each component, the materials that are employed along with their property limitations. This package design is popular with digital IC manufacturers primarily because its production can be highly automated.

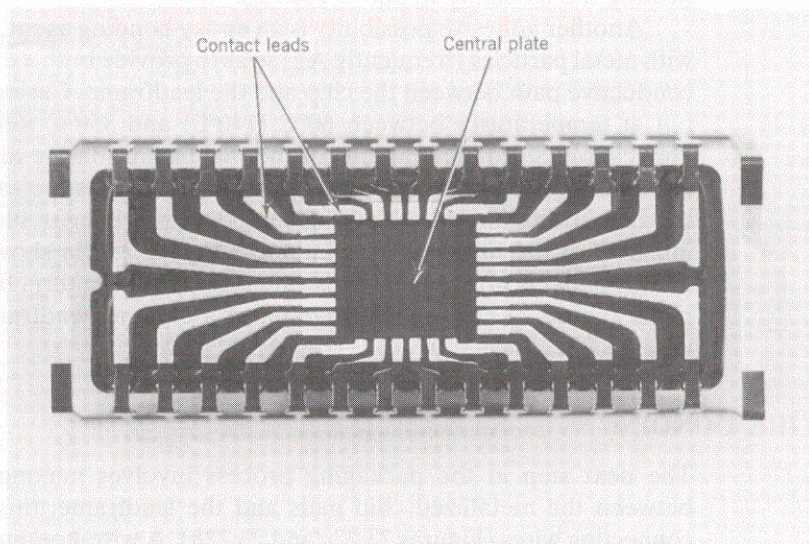
23.13 LEADFRAME DESIGN AND MATERIALS

The leadframe, as the name suggests, is a frame to which electrical leads may be made from the IC chip. A photograph of a leadframe-type package is shown in Figure 23.21. In essence, the leadframe consists of a central plate onto which the die is mounted, and an array of contact leads to which wire connections may be made from the contact pads on the chip. Some leadframe designs also call for a substrate onto which the die is mounted, which substrate is, in turn, bonded to the central plate. During the packaging process, and after the chip has been attached to the central plate (a procedure termed *die bonding*), the contact pads on the IC chip are cleaned, wires are attached to both the contact pads and the leadframe leads (called *wire bonding*), and, finally, this package is encapsulated in a protective enclosure so as to seal out moisture, dust, and other contaminants. This procedure is called *hermetic sealing*.

There are some rather stringent requirements on the properties of the material to be used for the leadframe; these are as follows: (1) The leadframe material must have a high electrical conductivity, inasmuch as there will be current passage through its leads. (2) The leadframe, the die attach central plate, substrate (if present), and die-bonding adhesive must also be thermally conductive so as to facilitate the dissipation of heat generated by the IC. (3) A coefficient of thermal expansion comparable to that of Si is highly desirable; a thermal expansion mismatch could destroy the integrity of the bond between the IC and the central plate as a result of thermal cycling during normal operation. (4) The leadframe material and sub-

FIGURE 23.21

Photograph of a leadframe on which the central plate and contact leads are labeled. 2×. (Leadframe supplied by National Semiconductor Corporation. Photograph by Dennis Haynes.)



strate must also adhere to the die-bonding adhesive, and the adhesive and substrate must also be electrically conductive. (5) A secure and electrically conductive joint between the leadframe and the connecting wires must be possible. (6) The leadframe must be resistant to oxidation and retain its mechanical strength during any thermal cycling that may accompany the die-bonding and encapsulation procedures. (7) The leadframe must also withstand corrosive environments at high temperatures and high humidities. (8) It must be possible to mass produce the leadframes economically. Normally, they are stamped from thin metal sheets.

A parenthetical comment is in order relative to the electrical characteristics of the substrate and die-bonding adhesive. In the preceding paragraph it was noted that the materials used for these two leadframe components must be electrically conductive. This is inconsistent with the ceramic materials used for packaging substrates which, as discussed in Section 14.18, must be electrical insulators. This discrepancy is resolved when it is realized that some package designs call for grounding of the IC chip through the substrate, whereas for other designs, grounding is through the contact wires.

Several alloys have been used for the leadframe with varying degrees of success. The most commonly used materials are copper-based alloys; the compositions, electrical and thermal conductivities, and coefficients of thermal expansion for two of the most popular ones (C19400 and C19500) are listed in Table 23.6. For the most part, they satisfy the criteria listed in the preceding paragraph. Also listed in the table are the compositions of two other alloys (Kovar and Alloy 42) that have been used extensively in leadframes. The desirability of these latter two alloys lies in their relatively low coefficients of thermal expansion, which are closely matched to that of Si [i.e., $2.5 \times 10^{-6} (\text{°C})^{-1}$]. However, from Table 23.6 it may also be noted that both electrical and thermal conductivities for Kovar and Alloy 42 are inferior to the conductivity values for the C19400 and C19500 alloys.

23.14 DIE BONDING

The die-bonding operation consists of attaching the IC chip to the central supporting leadframe plate. For the copper alloys noted in Table 23.6, attachment may be made using a gold–silicon eutectic solder; however, melting of the solder requires heating the assembly to 500°C (900°F).

Another adhesive possibility is an epoxy bonding agent, which is normally filled with metal particles (frequently Ag) so as to provide both a thermally and electrically conductive path between the chip and the leadframe. Curing of the epoxy is carried out at temperatures between 60°C (140°F) and 350°C (660°F) depending on the application. Since the amounts of thermal expansion are different for the Cu alloy leadframe plate and Si chip, the epoxy adhesive must be capable of absorbing any thermal strains produced during temperature changes such that the mechanical integrity of the junction is maintained. Figure 23.22a shows a schematic diagram of a chip that is bonded to a substrate layer that is, in turn, bonded to the leadframe plate. Figure 23.22b is a photograph of a chip, its leadframe, and the connecting wires.

23.15 WIRE BONDING

The next step in the packaging process involves making electrical connections between the metallized chip pads and the leadframe; this is accomplished using connecting wires (Figures 23.22a and 23.22b). A wire-bonding procedure is normally

Table 23.6 Designations, Compositions, Electrical and Thermal Conductivities, and Coefficients of Thermal Expansion for Common IC Leadframe Alloys

Alloy Designation	Composition (wt%)				Electrical Conductivity [$10^8 (\Omega\text{-m})^{-1}$]	Thermal Conductivity (W/m-K)	Coefficient of Thermal Expansion ^a [$10^{-6} (^\circ\text{C})^{-1}$]
	Fe	Ni	Co	Cu			
C19400	2.35			Balance	39.4	260	16.3
				0.03 P, 0.12 Zn, 0.03 Pb (max)			
C19500	1.5		0.8	Balance	29.1	200	16.9
Kovar (ASTM F15)	54	29	17	0.6 Sn, 0.03 P	2.0	17	5.1
Alloy 42 (ASTM F30)	58	42			1.4	12	4.9

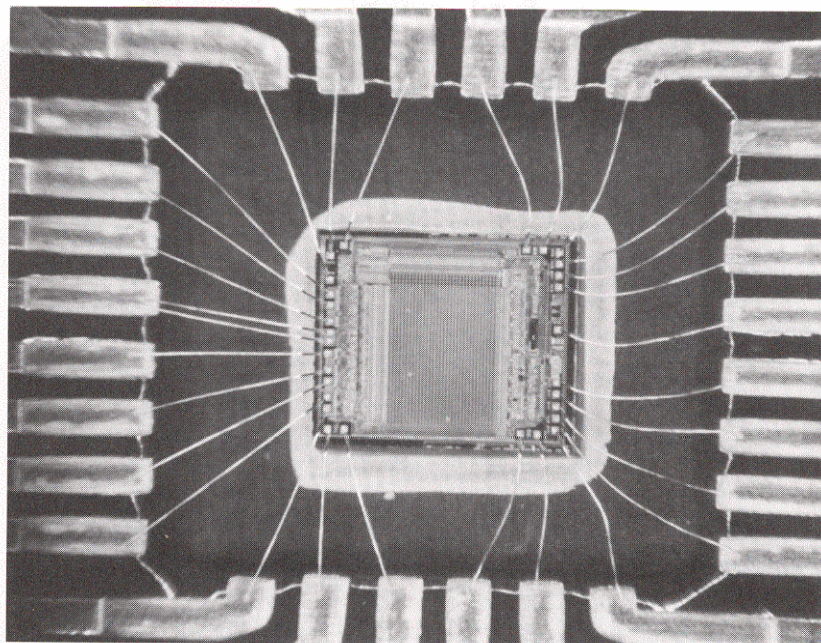
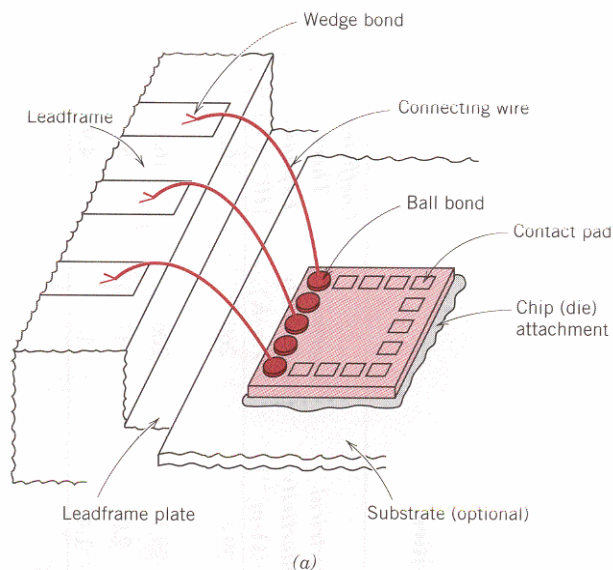
^a Coefficient of thermal expansion values are averages measured between 20°C and 300°C.

FIGURE 23.22 (a)

Schematic diagram showing the IC chip, its attachment to the substrate (or leadframe plate), and the connecting wires that run to the leadframe contact leads. (Adapted from *Electronic Materials Handbook*, Vol. 1, *Packaging*, C. A. Dostal, editor, ASM International, 1989, p. 225.)

(b) Photograph showing a portion of a leadframe package.

Included is the IC chip along with its connecting wires. One end of each wire is bonded to a chip pad; the other wire extremity is bonded to a leadframe contact lead. $7\times$. (Photograph courtesy of National Semiconductor Corporation.)



carried out using a microjoining operation, since very fine wires are used to make the connections. Wire bonding is the slow step in the packaging process because several hundred wires may need to be installed; this procedure is usually automated.

Several important considerations must be taken into account relative to the choice of wire alloy. Of course, a high electrical conductivity is the prime prerequisite. In addition, consideration must be given to the ability of the alloy to bond, by welding or brazing, with both the Al alloy at the chip pad and the Cu alloy on the leadframe; the formation of a microjoint that is both mechanically and electrically stable is an absolute necessity.

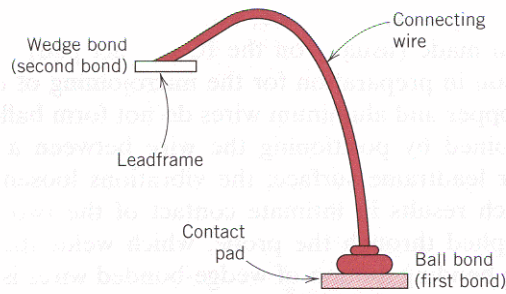
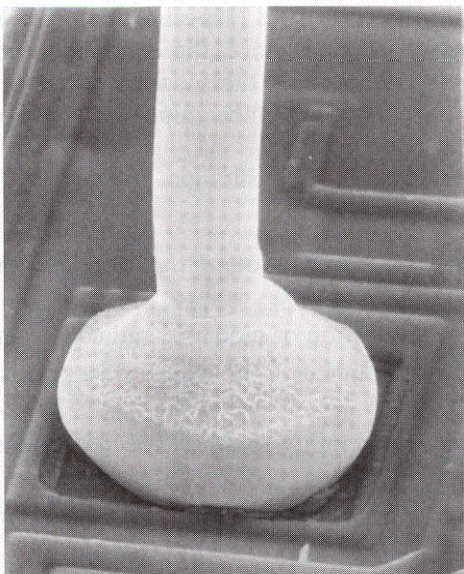


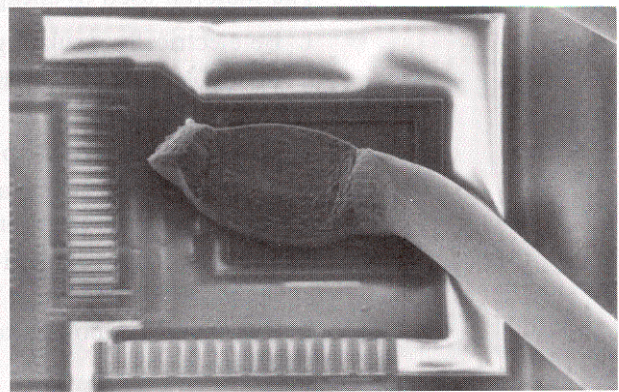
FIGURE 23.23 Schematic diagram showing a connecting wire that is ball bonded to the IC contact pad and wedge bonded to the leadframe. (Adapted from *Electronic Materials Handbook*, Vol. 1, *Packaging*, C. A. Dostal, editor, ASM International, 1989, p. 225.)

The most commonly used wire material is gold—actually a gold alloy containing a small amount of beryllium—copper that is added to inhibit grain growth. Gold wires are round and have diameters that are typically $18\text{ }\mu\text{m}$ (0.0007 in.), $25\text{ }\mu\text{m}$ (0.001 in.), or $50\text{ }\mu\text{m}$ (0.002 in.). Less costly Cu and Al have also been employed for contact wires. Prior to making the microjoint, regions of the chip pad and leadframe surfaces at which the junctions are to be made may be coated with Au so as to improve bondability. During the actual microjoining process, one wire end is brought into the vicinity of one of the joint regions using a special tool. This wire end is then melted with a spark or flame heat source.

Two different types of microjoints are possible: ball and wedge. Figure 23.23 is a schematic diagram showing a connecting wire having a ball microjoint at its contact pad end and a wedge microjoint at the leadframe connection. Ball joints are possible for gold wires since the melted wire end forms into a small ball because of the high surface tension of gold. Bonding of this molten ball with the contact pad or leadframe is accomplished by making mechanical contact with the bonding surface while both wire and surface are subjected to ultrasonic vibrations. A scanning electron micrograph of a ball microjoint is shown in Figure 23.24a. This type of



(a)



(b)

FIGURE 23.24 Scanning electron micrographs of (a) a ball bond ($475\times$), and (b) a wedge bond ($275\times$). (Photographs courtesy of National Semiconductor Corporation.)

microjoint is especially desirable since, after the first of the two microjoints for each wire has been made (usually on the IC contact pad), the wire may then be bent in any direction in preparation for the microjoining of its other extremity.

The ends of copper and aluminum wires do not form balls upon melting. They are wedge microjoined by positioning the wire between a vibrating probe and the contact pad or leadframe surface; the vibrations loosen and remove surface contaminants, which results in intimate contact of the two surfaces. An electric current is then applied through the probe, which welds the wire to the surface. Unfortunately, the bending motion of wedge-bonded wires is restricted to a single direction. Gold wires may also be bonded using wedge microjoints. Figure 23.24*b* is a scanning electron micrograph of a wedge microjoint.

There are other considerations relative to wire bonding that deserve mentioning. Microjunction alloy combinations that form intermetallic phases should be avoided because these phases are normally brittle and yield microjoints lacking long-term mechanical stability. For example, Au and Al may react at elevated temperatures to form AuAl_2 , termed the “purple plague”; this compound is not only very brittle (and purple), but also highly electrically resistive. Furthermore, mechanical integrity at each microjoint is important so as to (1) withstand vibrations that the package may experience, and (2) survive thermal stresses that are generated as the packaging materials change temperature.

23.16 PACKAGE ENCAPSULATION

The microelectronic package, as now constituted, must be provided some type of protection from corrosion, contamination, and damage during handling and while in service. The wire interconnection microjunctions are extremely fragile and may be easily damaged. Especially vulnerable to corrosion are the narrow Al circuit paths that have been metallized onto the surface of the IC chip; even the slightest corrosion of these elements will impair the operation of the chip. These Al-metallized layers experience corrosion when atmospheric moisture in which even minute concentrations of ionic contaminants are dissolved (especially chlorine and phosphorus) condenses on the chip surface. Furthermore, the corrosive reactions are accelerated as a consequence of electric currents that pass through these circuit paths. In addition, any sodium (as Na^+) that gets on the chip surface will eventually diffuse into the chip and destroy its operation.

The material used to encapsulate the package should:

1. Be electrically insulating;
2. Be easily molded to the desired shape around the chip die and its wire leads;
3. Be highly impervious to the penetration of moisture and contaminants;
4. Be able to form strong adhesive bonds with the chip surface, wires, and other leadframe components;
5. Exhibit mechanical and chemical stability for the expected lifetime of the package;
6. Not require exposure to excessively high temperatures during installation;
7. Have a coefficient of thermal expansion similar to those of other package components so as to avoid thermal stresses capable of fracturing the wire leads.

Figure 23.25 shows a schematic diagram of an encapsulated IC package.

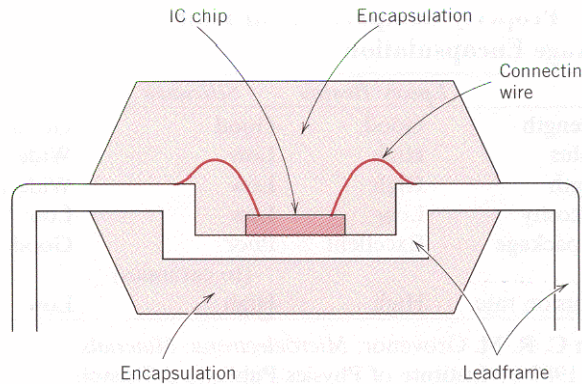


FIGURE 23.25 Schematic diagram showing an encapsulated IC leadframe package. (Adapted from *Electronic Materials Handbook*, Vol. 1, *Packaging*, C. A. Dostal, editor, ASM International, 1989, p. 241.)

Both ceramic and polymeric materials are used to encapsulate IC packages; of course each of these material types has its own set of assets and liabilities. Ceramics are extremely resistant to moisture penetration and are chemically stable and chemically inert. Glasses are the most commonly utilized ceramic materials. The principal disadvantage of glass is the requirement that it be heated to moderately high temperatures to lower its viscosity to the point where it will flow around and make intimate contact with all of the wires that are microjoined to the chip surface. Some common glass constituents should be avoided (notably Na_2O and K_2O) since volatile cation species (Na^+ and K^+) may be emitted from the molten glass. These species are notorious in accelerating corrosion reactions, and the ions will degrade the chip performance.

Polymeric materials are used in the largest volume for packaging encapsulation because they are not as costly as the ceramics, and they may be produced in a low-viscosity state at lower temperatures. Epoxies and polyurethanes are commonly used, with the former being the most common. However, these materials have a tendency to absorb water and do not form moisture-tight bonds with the lead wires. Some of these polymers require curing at a temperature on the order of 150°C , and during cooling to room temperature will shrink more than other package components to which they are attached. This difference in amounts of contraction can give rise to mechanical strains of sufficient magnitude to damage the connecting wires as well as other electronic components. The addition of appropriate fillers (such as fine silica or alumina particles) to the polymer can alleviate this problem but often has undesirable electrical consequences. A comparison of the important encapsulation characteristics of four different polymer types is given in Table 23.7.

23.17 TAPE AUTOMATED BONDING

Another packaging design, *tape automated bonding* (or *TAB*), a variation of the leadframe discussed above, has found widespread use by virtue of its low cost. The tape-bonded package consists of a thin and flexible polyimide polymer backing film substrate; onto this substrate surface is patterned an array of copper “finger” high-conductivity conduction paths similar in configuration to the contact leads for the conventional leadframe. A schematic diagram of a tape-bonded film leadframe is shown in Figure 23.26.

Mechanical support for the assembly is provided by the polyimide film, onto which the die is bonded using an adhesive. Polyimide strip widths are typically 35 mm (1.38 in.), and sprocket holes are incorporated along opposing edges so as to facilitate movement and positioning of the TAB leadframes. Literally thousands

Table 23.7 Property Comparisons of Four Classes of Polymers Used for IC Package Encapsulation

	Epoxy Resins	Silicones	Polyurethanes	Polysulphides
Dielectric strength	Good	Good	Good	Good
Elastic modulus	High	Low	Wide range	Low
Tensile strength	High	Low	Wide range	—
Precursor viscosity	Low	Low	Low	High
Adhesion to package	Excellent	Poor (to ceramics)	Good	Good
Moisture diffusion rate	High	High	Low	Very low

Source: From C. R. M. Grovenor, *Microelectronic Materials*.
Copyright © 1989 by Institute of Physics Publishing, Bristol.

of these individual units, attached end to end, are spooled onto reels in preparation for automated processing.

The copper fingers are extremely narrow and positioned close together. Separation distances of the inner contact leads are on the order of 50 μm , which is much smaller than is possible for the stamped leadframe. Furthermore, each die chip contact pad is microjoined directly to one of these copper fingers, which eliminates the need for any connecting wires. The copper fingers are very thin, so that, for this direct bonding to be achieved, the chip pad bonding sites must be raised above the metallized coating. This is accomplished using “solder bumps,” which are normally layers of gold (or gold-plated copper) approximately 25 μm thick. Schematic representations illustrating this attachment design are presented in Figure 23.27. The finger contacts are bonded to these raised bumps by soldering using a thermal-compression bonding tool. This tape-bonding design is fully automated in that all of the hundred or so microjoints can be made in a single step, a feature not possible with leadframes that require multiple wire-bonding operations.

The packaging operation for the TAB leadframe is completed, as with the stamped leadframe, by encapsulation of the assembly (i.e., tape leadframe and its

FIGURE 23.26
Schematic diagram of a complete tape-bonded (TAB) leadframe. (From *Electronic Materials Handbook*, Vol. 1, *Packaging*, C. A. Dostal, editor, ASM International, 1989, p. 233.)

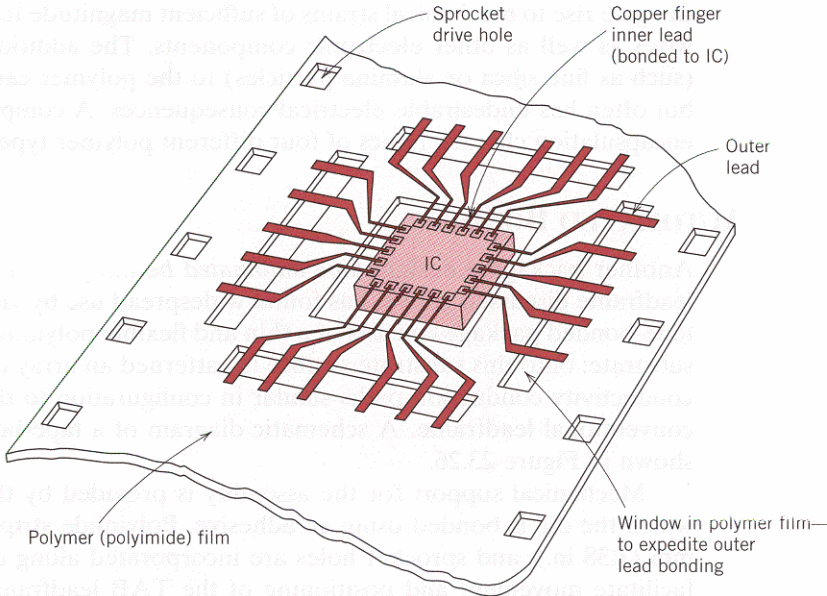
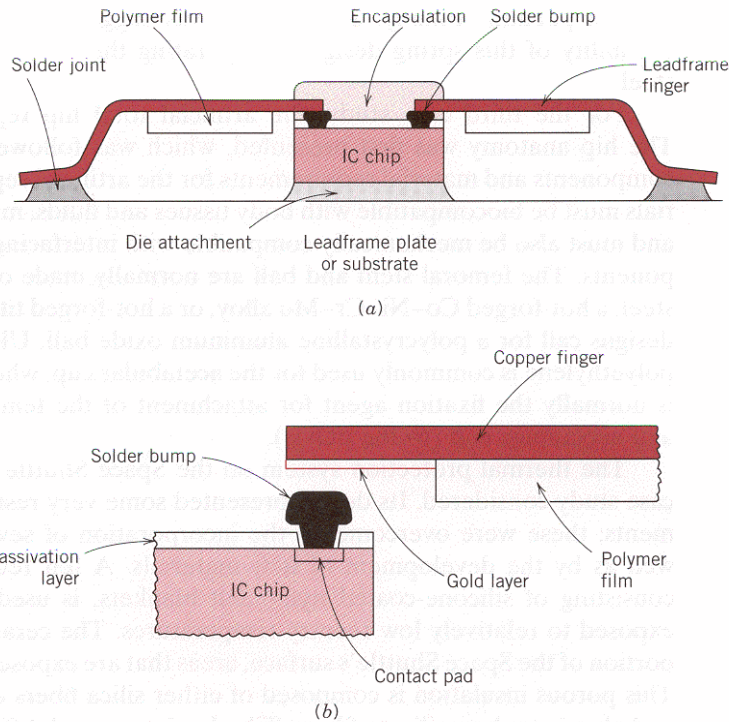


FIGURE 23.27

Schematic diagrams showing (a) the cross section of an encapsulated TAB leadframe package, and (b) how bonding between the IC chip and a copper finger is achieved with a solder bump. (Adapted from *Electronic Materials Handbook*, Vol. 1, Packaging, C. A. Dostal, editor, ASM International, 1989, pp. 233, 234.)



attached chip) within a fluid polymeric material that subsequently cures so as to form a protective shield. Protruding from this package are the copper finger conducting paths to which external electrical connections are made. Furthermore, excess heat generated by the chip must be dissipated along these copper fingers inasmuch as the polymer tape backing does not provide an effective thermal conduction path because of its low thermal conductivity.

The ultimate design goal of the IC package is to allow for the proper electrical operation of the packaged device. As frequencies and computing speeds creep ever higher, the mechanical and electrical design considerations of the package design must become more and more integrated. The overall electrical performance of the package is as important to the end user as the overall reliability.

SUMMARY

In this chapter, we have illustrated the protocol of materials selection using five diverse examples. For the first case, a torsionally stressed cylindrical shaft, an expression for strength performance index was derived; then, using the appropriate materials selection chart, a preliminary candidate search was conducted. From the results of this search, several candidate engineering materials were ranked on both strength-per-unit mass and cost bases. Other factors that are relevant to the decision-making process were also discussed.

A stress analysis was next performed on a helical spring, which was then extended to an automobile valve spring. It was noted that the possibility of fatigue failure was crucial to the performance of this spring application. The shear stress amplitude was computed, the magnitude of which was almost identical to the calculated fatigue limit for a chrome–vanadium steel that is commonly used for valve springs. It was noted that the fatigue limit of valve springs is often enhanced

by shot peening. Finally, a procedure was suggested for assessing the economic feasibility of this spring design incorporating the shot-peened chrome–vanadium steel.

For the third case study, the artificial total hip replacement was explored. The hip anatomy was first presented, which was followed by a discussion of the components and material requirements for the artificial replacement. Implant materials must be biocompatible with body tissues and fluids, must be corrosion resistant, and must also be mechanically compatible with interfacing replacement/body components. The femoral stem and ball are normally made of a cold-worked stainless steel, a hot-forged Co–Ni–Cr–Mo alloy, or a hot-forged titanium alloy. Some recent designs call for a polycrystalline aluminum oxide ball. Ultrahigh molecular weight polyethylene is commonly used for the acetabular cup, whereas acrylic bone cement is normally the fixation agent for attachment of the femoral stem (to the femur) and acetabular cup (to the pelvis).

The thermal protection system on the Space Shuttle was the fourth materials case study considered. Its design presented some very restrictive materials requirements; these were overcome by the incorporation of several different systems as well as by the development of new materials. A felt reusable surface insulation, consisting of silicone-coated nylon felt blankets, is used for those surface areas exposed to relatively low reentry temperatures. The ceramic tiles cover the major portion of the Space Shuttle's surface, areas that are exposed to higher temperatures. This porous insulation is composed of either silica fibers or a combination of silica and aluminum borosilicate fibers. Tiles having several different strengths, densities, and thermal properties are fabricated for utilization at the various locations. A thin glass surface coating is applied to each tile so as to improve either its reflectance or emissive characteristics. Those surface regions of the Shuttle that experience the highest reentry temperatures are constructed of a reinforced carbon–carbon composite that is coated with a thin layer of silicon carbide.

Materials utilized for the integrated circuit package incorporating the leadframe design were the topic of the final case study. An IC chip is bonded to the leadframe plate using either a eutectic solder or an epoxy resin. The leadframe material must be both electrically and thermally conductive, and, ideally, have a coefficient of thermal expansion that matches the IC chip material (i.e., silicon or gallium arsenide); copper alloys are commonly used leadframe materials. Very thin wires (preferably of gold, but often of copper or aluminum) are used to make electrical connections from the microscopic IC chip contact pads to the leadframe. Ultrasonic microjoining welding/brazing techniques are used where each connection joint may be in the form of either a ball or wedge. The final step is package encapsulation, wherein this leadframe–wire–chip assembly is encased in a protective enclosure. Ceramic glasses and polymeric resins are the most common encapsulation materials. Resins are less expensive than glasses and require lower encapsulation temperatures; however, glasses normally offer a higher level of protection.

REFERENCES

- General** ASM Handbook, Vol. 20, *Materials Selection and Design*, ASM International, Materials Park, OH, 1997.
- Ashby, M. F., *Materials Selection in Mechanical Design*, Pergamon Press, Oxford, 1992.

Budinski, K. G., *Engineering Materials: Properties and Selection*, 5th edition, Prentice Hall, Inc., Englewood Cliffs, NJ, 1995.

Creyke, W. E. C., I. E. J. Sainsbury, and R. Morrell, *Design with Nonductile Materials*, Applied Science Publishers, London, 1982.

Dieter, G. E., *Engineering Design, A Materials and Processing Approach*, 2nd edition, McGraw-Hill Book Company, New York, 1991.

Farag, M. M., *Materials Selection for Engineering Design*, Prentice Hall, Inc., Upper Saddle River, NJ, 1997.

Lewis, G., *Selection of Engineering Materials*, Prentice Hall, Inc., Englewood Cliffs, NJ, 1990.

Mangonon, P. L., *The Principles of Materials Selection for Engineering Design*, Prentice Hall, Saddle River, NJ, 1999.

Optimization of Strength

Ashby, M. F. and D. R. H. Jones, *Engineering Materials I, An Introduction to Their Properties and Applications*, 2nd edition, Pergamon Press, Oxford, 1996.

Automotive Valve Springs

Edwards, K. S., Jr. and R. B. McKee, *Fundamentals of Mechanical Component Design*, Chapter 18, McGraw-Hill Book Company, New York, 1991.

Society of Automotive Engineers Handbook, 1991 edition, Section 6, Society of Automotive Engineers, Inc., 1991.

Artificial Hip Replacements

Williams, D. F. (Editor), *Biocompatibility of Orthopedic Implants*, Vol. I, CRC Press, Inc., Boca Raton, FL, 1982.

Pilliar, R. M., "Manufacturing Processes of Metals: The Processing and Properties of Metal Implants," *Metal and Ceramic Biomaterials*, P. Ducheyne and G. Hastings (Editors), CRC Press, Inc., Boca Raton, FL, 1984.

Thermal Protection System on the Space Shuttle Orbiter

Korb, L. J., C. A. Morant, R. M. Calland, and C. S. Thatcher, "The Shuttle Orbiter Thermal Protection System," *American Ceramic Society Bulletin*, Vol. 60, No. 11, 1981, pp. 1188–1193.

Cooper, P. A. and P. F. Holloway, "The Shuttle Tile Story," *Astronautics and Aeronautics*, Vol. 19, No. 1, 1981, pp. 24–36.

Gordon, M. P., *The Space Shuttle Orbiter Thermal Protection System, Processing Assessment, Final Report*, http://ihm.arc.nasa.gov/repair/shuttle_report/index.html.

Integrated Circuit Packaging

Electronic Materials Handbook, Vol. I, Packaging, ASM International, Materials Park, OH, 1989.

Grovenor, C. R. M., *Microelectronic Materials*, Institute of Physics Publishing, Bristol, 1989.

QUESTIONS AND PROBLEMS

Design Problems

23.D1 (a) Using the procedure as outlined in Section 23.2 ascertain which of the metal alloys listed in Appendix B (and also the database on the CD-ROM), have torsional strength performance indices greater than 12.5 (in SI units), and, in addition, shear strengths greater than 300 MPa. **(b)** Also using the cost database (Appendix C), conduct a cost analysis in the same manner as Section 23.2. For those materials that satisfy the criteria noted in part a, and,

on the basis of this cost analysis, which material would you select for a solid cylindrical shaft? Why?

23.D2 In a manner similar to the treatment of Section 23.2, perform a stiffness-to-mass performance analysis on a solid cylindrical shaft that is subjected to a torsional stress. Use the same engineering materials that are listed in Table 23.1. In addition, conduct a material cost analysis. Rank these materials both on the basis of mass of material required and material cost. For glass

and carbon fiber-reinforced composites, assume that the shear moduli are 8.6 and 9.2 GPa, respectively.

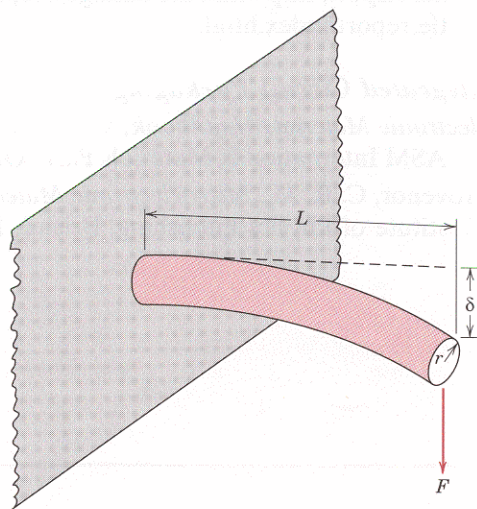
- 23.D3 (a)** A cylindrical cantilever beam is subjected to a force F , as indicated in the figure below. Derive strength and stiffness performance index expressions analogous to Equations 23.9 and 23.11 for this beam. The stress imposed on the unfixed end σ is

$$\sigma = \frac{FLr}{I} \quad (23.24)$$

L , r , and I are, respectively, the length, radius, and moment of inertia of the beam. Furthermore, the beam-end deflection δ is

$$\delta = \frac{FL^3}{3EI} \quad (23.25)$$

where E is the modulus of elasticity of the beam.



- (b)** From the properties database presented in Appendix B (or on the CD-ROM), select those metal alloys with stiffness performance indices greater than 3.0 (in SI units).

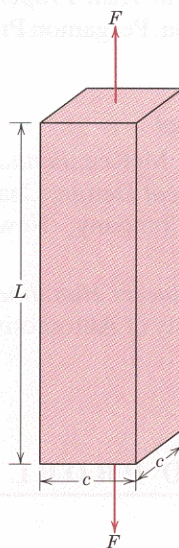
- (c)** Also using the cost database (Appendix C), conduct a cost analysis in the same manner as Section 23.2. Relative to this analysis and that in part b, which alloy would you select on a stiffness-per-mass basis?

- (d)** Now select those metal alloys having strength performance indices greater than 18.0 (in SI units), and rank them from highest to lowest P .

- (e)** And, using the cost database, rank the materials in part d from least to most costly. Relative to this analysis and that in part d, which alloy would you select on a strength-per-mass basis?

- (f)** Which material would you select if both stiffness and strength are to be considered relative to this application? Justify your choice.

- 23.D4 (a)** A bar specimen having a square cross section of edge length c is subjected to a uniaxial tensile force F , as shown in the following figure. Derive strength and stiffness performance index expressions analogous to Equations 23.9 and 23.11 for this bar.



- (b)** From the properties database presented in Appendix B (or on the CD-ROM), select those metal alloys with stiffness performance indices greater than 26.3 (in SI units).

- (c)** Also using the cost database (Appendix C), conduct a cost analysis in the same manner as Section 23.2. Relative to this analysis and that in part b, which alloy would you select on a stiffness-per-mass basis?

(d) Now select those metal alloys having strength performance indices greater than 100 (in SI units), and rank them from highest to lowest P .

(e) And, using the cost database, rank the materials in part d from least to most costly. Relative to this analysis and that in part d, which alloy would you select on a strength-per-mass basis?

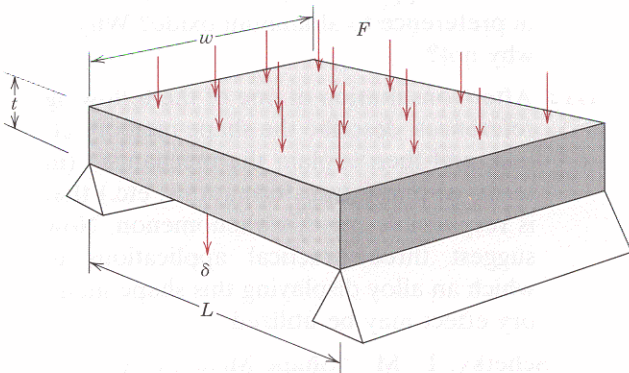
(f) Which material would you select if both stiffness and strength are to be considered relative to this application? Justify your choice.

23.D5 Consider the plate shown below that is supported at its ends and subjected to a force F that is uniformly distributed over the upper face as indicated. The deflection δ at the $L/2$ position is given by the expression

$$\delta = \frac{5FL^3}{32Ewt^3} \quad (23.26)$$

Furthermore, the tensile stress at the underside and also at the $L/2$ location is equal to

$$\sigma = \frac{3FL}{4wt^2} \quad (23.27)$$



(a) Derive stiffness and strength performance index expressions analogous to Equations 23.9 and 23.11 for this plate. (Hint: solve for t in these two equations, and then substitute the resulting expressions into the mass equation, as expressed in terms of density and plate dimensions.)

(b) From the properties database in Appendix B (or on the CD-ROM), select

those metal alloys with stiffness performance indices greater than 1.50 (in SI units)

(c) Also using the cost database (Appendix C), conduct a cost analysis in the same manner as Section 23.2. Relative to this analysis and that in part b, which alloy would you select on a stiffness-per-mass basis?

(d) Now select those metal alloys having strength performance indices greater than 6.0 (in SI units), and rank them from highest to lowest P .

(e) And, using the cost database, rank the materials in part d from least to most costly. Relative to this analysis and that in part d, which alloy would you select on a strength-per-mass basis?

(f) Which material would you select if both stiffness and strength are to be considered relative to this application? Justify your choice.

23.D6 A spring having a center-to-center diameter of 15 mm (0.6 in.) is to be constructed of cold-worked ($\frac{1}{4}$ hard) 304 stainless steel wire that is 2.0 mm (0.08 in.) in diameter; this spring design calls for ten coils.

(a) What is the maximum tensile load that may be applied such that the total spring deflection will be no more than 5 mm (0.2 in)?

(b) What is the maximum tensile load that may be applied without any permanent deformation of the spring wire? Assume that the shear yield strength is 0.6 σ_y , where σ_y is the yield strength in tension.

23.D7 You have been asked to select a material for a spring that is to be stressed in tension. It is to consist of 8 coils, and the coil-to-coil diameter called for is 12 mm; furthermore, the diameter of the spring wire must be 1.75 mm. Upon application of a tensile force of 30 N, the spring is to experience a deflection of no more than 10 mm, and not plastically deform.

(a) From those materials included in the database in Appendix B (or on the CD-ROM), make a list of those candidate materials that meet the above criteria. As-

sume that the shear yield strength is $0.6\sigma_y$, where σ_y is the yield strength in tension, and that the shear modulus is equal to $0.4E$, E being the modulus of elasticity.

(b) Now, from this list of candidate materials, select the one you would use for this spring application. In addition to the above criteria, the material must be relatively corrosion resistant, and, of course, capable of being fabricated into wire form. Justify your decision.

- 23.D8** A spring having 10 coils and a coil-to-coil diameter of 0.4 in. is to be made of cold-drawn steel wire. When a tensile load of 12.9 lb_f is applied the spring is to deflect no more than 0.80 in. The cold drawing operation will, of course, increase the shear yield strength of the wire, and it has been observed that τ_y (in ksi) depends on wire diameter d (in in.) according to

$$\tau_y = \frac{63}{d^{0.2}} \quad (23.28)$$

If the shear modulus for this steel is 11.5×10^6 psi, calculate the minimum wire diameter required such that the spring will not plastically deform when subjected to the above load.

- 23.D9** A helical spring is to be constructed from a 4340 steel. The design calls for 12 coils, a coil-to-coil diameter of 12 mm, and a wire diameter of 2 mm. Furthermore, in response to a tensile force of 27 N, the total deflection is to be no more than 3.5 mm. Specify a heat treatment for this 4340 steel wire in order for the spring to meet the above criteria. Assume a shear modulus of 80 GPa for this steel alloy, and that $\tau_y = 0.6\sigma_y$.

- 23.D10** Using the *E-Z Solve* software included on the CD-ROM that accompanies this book, construct a routine for the automobile valve spring (Section 23.5) that allows the user to specify the number of effective coils (N), the spring coil-to-coil diameter (D), and the wire cross-section diameter (d), and calculates the fatigue limit (τ_{al}) as well as the actual stress amplitude (τ_{aa}). Incorporate into this routine values cited for installed and maximum deflections per coil

(i.e., $\delta_{ic} = 0.24$ in. and $\delta_{mc} = 0.54$ in.), as well as for the shear modulus of steel ($G = 11.5 \times 10^6$ psi).

- 23.D11** You have been asked to select a metal alloy to be used as leadframe plate in an integrated circuit package that is to house a silicon chip.

(a) Using the database in Appendix B (or on the CD-ROM) list those materials that are electrically conductive [$\sigma > 10 \times 10^6$ ($\Omega\text{-m}$)⁻¹], have linear coefficients of thermal expansion of between 2×10^{-6} and 10×10^{-6} ($^{\circ}\text{C}$)⁻¹, and thermal conductivities of greater than 100 W/m-K. On the bases of properties and cost, would you consider any of these materials in preference to those listed in Table 23.6? Why or why not?

(b) Repeat this procedure for potential insulating leadframe plate materials that must have electrical conductivities less than 10^{-10} ($\Omega\text{-m}$)⁻¹, as well as coefficients of thermal expansion between 2×10^{-6} and 10×10^{-6} ($^{\circ}\text{C}$)⁻¹, and thermal conductivities of greater than 30 W/m-K. On the bases of properties and cost (Appendix C), would you consider any of the materials listed in Appendix B (or on the CD-ROM) in preference to aluminum oxide? Why or why not?

- 23.D12** After consultation of one of the following references, describe the shape memory effect, and then explain the mechanism (in terms of phase transformations, etc.) that is responsible for this phenomenon. Now suggest three practical applications in which an alloy displaying this shape memory effect may be utilized.

Schetky, L. M., "Shape-Memory Alloys," *Scientific American*, Vol. 241, No. 5, November 1979, pp. 74–82.

"Shape-Memory Alloys—Metallurgical Solution Looking for a Problem," *Metalurgia*, Vol. 51, No. 1, January 1984, pp. 26–29.

- 23.D13** Write an essay on the replacement of metallic automobile components by polymers and composite materials. Address the following issues: (1) Which automotive

components (e.g., crankshaft) now use polymers and/or composites? (2) Specifically what materials (e.g., high-density polyethylene) are now being used? (3) What are the reasons for these replacements?

- 23.D14** Perform a case study on material usage for the compact disc, after the manner of those studies described in this chapter. Begin with a brief description of the mechanism by which sounds are stored and then reproduced. Then, cite all of the requisite material properties for this application; finally, note which material is most commonly utilized, and the rationale for its use.
- 23.D15** One of the critical components of our modern video cassette recorders (VCRs) is the magnetic recording/playback head. Write an essay in which you address the following issues: (1) the mechanism by which the head records and plays back video/audio signals; (2) the requisite properties for the material from which the head is manufactured; then (3) present at least three likely candidate materials, and the property values for each that make it a viable candidate.
- 23.D16** Another group of new materials are the metallic glasses (or amorphous metals).

Write an essay about these materials in which you address the following issues: (1) compositions of some of the common metallic glasses; (2) characteristics of these materials that make them technologically attractive; (3) characteristics that limit their utilization; (4) current and potential uses; and (5) at least one technique that is used to produce metallic glasses.

- 23.D17** The transdermal patch has recently become popular as a mechanism for delivering drugs into the human body.
- (a) Cite at least one advantage of this drug-delivery system over oral administration using pills and caplets.
- (b) Note the limitations on drugs that are administered by transdermal patches.
- (c) Make a list of the characteristics required of materials (other than the delivery drug) that are incorporated in the transdermal patch.
- 23.D18** Glass, aluminum, and various plastic materials are utilized for beverage containers (page 1). Make a list of the advantages and disadvantages of using each of these three material types; include such factors as cost, recyclability, and energy consumption for container production.